Second-day road log: From Quemado Lake to Mangas Mountains, Omega, Quemado, Tejana Mesa and Red Hill, New Mexico and Springerville and Alpine, Arizona

Steven M. Cather, Richard M. Chamberlin, William C. McIntosh, James C. Witcher, James C. Ratte, and Orin J. Anderson

1994, pp. 47-77. https://doi.org/10.56577/FFC-45.47

in:

Mogollon Slope (West-Central New Mexico and East-Central Arizona), Chamberlin, R. M.; Kues, B. S.; Cather, S. M.; Barker, J. M.; McIntosh, W. C.; [eds.], New Mexico Geological Society 45th Annual Fall Field Conference Guidebook, 335 p. https://doi.org/10.56577/FFC-45

This page is intentionally left blank to maintain order of facing pages.

SECOND-DAY ROAD LOG FROM QUEMADO LAKE TO MANGAS MOUNTAINS, OMEGA, QUEMADO, TEJANA MESA AND RED HILL, NEW MEXICO, AND SPRINGERVILLE AND ALPINE, ARIZONA

STEVEN M. CATHER, RICHARD M. CHAMBERLIN, WILLIAM C. MCINTOSH, JAMES WITCHER, JAMES C. RATTÉ and ORIN J. ANDERSON

FRIDAY, SEPTEMBER 30, 1994

Assembly Point: East end of Quemado Lake Campground, 2.6 mi SE of Quemado Lake Dam on Forest Road 13.
Departure Time: 8:00 a.m.
Distance: 133.3 mi
Stops: 4

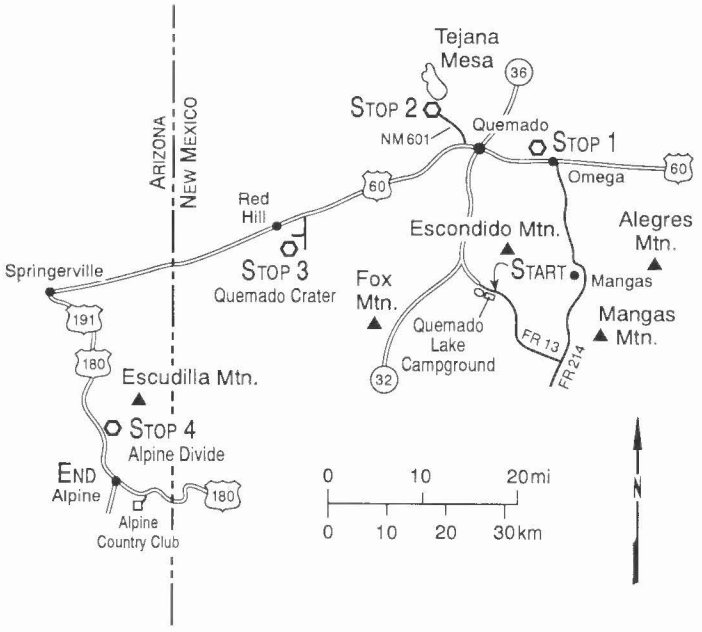

SUMMARY

Today's route traverses part of the northwestern margin of the late Eocene to late Oligocene Mogollon-Datil volcanic field in west-central New Mexico and eastern Arizona. Volcanic and sedimentary rocks of late Cenozoic age are also exposed along the field-trip route and will be discussed.

The route begins with a scenic loop through the Mangas Mountains. Stop 1 is an overlook area along US-60 west of Omega, where we will discuss petroleum exploration and regional seismic reflection profiles in the Mangas-Alegres Mountain area, and the hydrology of the Largo Creek drainage basin. At Stop 2 we will visit a fissure vent at El Porticito near the south end of Tejana Mesa to discuss the geochemistry and petrology of upper Tertiary volcanic rocks near Quemado and the planned coal mine east of Tejana Mesa. Quemado crater, a Quaternary maar/cinder cone complex just south of US-60 near Red Hill, is Stop 3 and the lunch stop. There we will discuss the volcanology of the crater and role of faults and fractures in the localization of late Cenozoic volcanoes in the region. Stop 4 is on the Alpine Divide north of Alpine, Arizona, where we will discuss the recent Alpine 1/Federal corehole and regional heat flow. After Stop 4, we will travel south to Alpine, Arizona to end the day's tour. Much of the geologic information presented here is from reconnaissance studies by Chamberlin et al. (1994b).

Mileage

0.0 East end of Quemado Lake Recreation Area, 2.6 mi southeast of Quemado Lake Dam on Forest Road (FR) 13. Head east, upstream, along El Caso Springs Canyon toward the Alpine meadows of Slaughter Mesa, approximately 5 mi from here. **0.1**

0.1 El Caso Peak at 1:30 is capped by lava flows of the Squirrel Springs Canyon Andesite, and the underlying andesite of San Antone Canyon. The andesite of San Antone Canyon is an aphanitic flow-banded mafic lava about 60 ft thick. Two coarsely porphyritic flows, each approximately 60 ft thick, comprise the Squirrel Springs Canyon Andesite. Vicks Peak Tuff (28.5 Ma), which locally occurs between these formations, is apparently absent here. **0.2**

0.3 Sign for Slaughter Mesa loop to NM-32, 26 mi. This road log takes the undesignated Mangas Mountain loop to US-60, 38 mi. **0.2**

0.5 Culvert; road crosses Canyon de Lolo which drains the south flank of Escondido Mountain. Sandstone cliff at 2:30 consists of massive light gray, crossbedded eolian sandstone assigned to the upper Oligocene sandstone of Escondido Mountain (Chamberlin and Harris, this volume). **0.1**

0.6 Junction with Baca Road on left. **Continue straight ahead on FR-13**. Baca Road parallels Canyon de Lolo to the south flank of Escondido Mountain. East-northeast- and east-trending normal faults that cut across Escondido Mountain locally *appear* to control the distribution of Squirrel Springs Canyon Andesite and the overlying Bloodgood Canyon Tuff, which suggests normal movement on these faults may have initiated as early as 26 to 28 Ma. Alternatively, these volcanic flows may have filled east-trending swales in the underlying dune deposits assigned to the sandstone of Escondido Mountain. In the latter case, local stratigraphic omission on the structurally high block would be fortuitous. **0.1**

0.7 Canyon wall exposure on left in sandstone of Escondido Mountain. Private road to El Caso Springs on right, just ahead. Low mesa at 2:00 is capped by Miocene Fence Lake Formation. High mesa at 12:00 is capped by upper Oligocene (ca. 26 Ma) basaltic andesite lava flows assigned to the Mangas Mountain Member of the Bearwallow Mountain Andesite. **0.2**

0.9 Outcrop at road level on left in upper Oligocene sandstone of Escondido Mountain, unconformably overlain by middle to upper Miocene Fence Lake Formation. Basal Fence Lake conglomerate contains abundant cobbles and boulders derived from the Bearwallow Mountain Andesite (dark gray basaltic andesite). Sparse clasts of light gray Bloodgood Canyon Tuff and coarsely porphyritic, Squirrel Springs Canyon Andesite are also present. **0.2**

1.1 Road crosses drainage of El Caso Springs Canyon at culvert. **0.4**

1.5 Road ascends onto upper surface of Fence Lake Formation, which here is only 40 ft above Quaternary valley fills along El Caso Springs Canyon. **0.5**

2.0 Road descends onto Quaternary valley fill that is inset against Fence Lake Formation. The Fence Lake is here locally inset against upper Oligocene volcanic strata that define its source area. **0.3**

2.3 Canyon wall on left is cut in flow-banded andesite of San Antone Canyon. **0.2**

2.5 Road rises onto poorly exposed terrace gravels assigned to the Fence Lake Formation. **0.2**

2.7 Jeep trail on left leads to Gooseberry Pit and upper reaches of El Caso Springs Canyon. **0.3**

3.0 Cattle guard. Road enters unnamed V-shaped canyon which heads near McKibben Tank on the north side of Slaughter Mesa. Fence Lake gravels terminate here, marking the local up-canyon limit of middle to late Miocene aggradation in this area. **0.2**

3.2 Low roadcut on right in medium gray, coarsely porphyritic and vesicular Squirrel Springs Canyon Andesite. The Squirrel Springs lavas typically contain about 20% phenocrysts of tabular plagioclase, 1–3 cm wide. **0.1**

3.3 Bloodgood Canyon Tuff, largely mantled with basaltic colluvium, is poorly exposed in low roadcut on right. Just ahead, road crosses colluvium-covered trace of east-northeast striking normal fault, downthrown approximately 60 ft to north. **0.1**

3.4 Cut on right in Squirrel Springs Canyon Andesite defines upthrown footwall of normal fault. Note light-colored bench of Bloodgood Canyon Tuff partially hidden in trees about 60 ft above road level on right. **0.4**

3.8 Vertical roadcut on right is in coarsely porphyritic Squirrel Springs Canyon Andesite (Figs. 2.1, 2.2). This locality may be used as an **optional stop** to view three regional volcanic formations locally well exposed along the western (right) side of the valley (Fig. 2.3). Whole-rock total-gas $^{40}Ar/^{39}Ar$ analyses of the Squirrel Springs Canyon Andesite and the basal Bearwallow Mountain Andesite collected from this site have yielded isochron ages of 28.8 ± 0.1 Ma and 26.1 ± 0.1 Ma, respectively (McIntosh and Chamberlin, this volume). The intervening Bloodgood Canyon Tuff, which was sampled 6 mi north of here in the same stratigraphic position, has yielded an $^{40}Ar/^{39}Ar$ age of 27.98 ± 0.09 Ma from sanidine. Field conference caravan will **not** stop here. **0.2**

4.0 Road on right leads to a small borrow pit 300 ft to west, which exposes 15 to 20 ft of trough-crossbedded granular sandstone apparently derived almost entirely from the underlying Squirrel Springs Canyon Andesite (Fig. 2.4). Local detailed mapping indicates that this granular sandstone fills an east-southeast trending (flowing?) paleovalley as much as 40 ft deep and a half mile wide. Except at the borrow pit, the granular sandstone is generally masked by gentle soil-covered slopes between resistant outcrops of the underlying Squirrel Springs Canyon Andesite and the overlying Bloodgood Canyon Tuff. The sandy matrix of the granular sandstone (Fig. 2.5) may have been recycled from contemporaneous eolian deposits, namely the sandstone of Escondido Mountain. **0.1**

4.1 On hillside to right, outcrops of the Squirrel Springs Canyon Andesite rise abruptly to meet with the base of the Bloodgood Canyon Tuff, about 30 ft higher on the slope. This relationship apparently defines the steeper

FIGURE 2.1. Roadcut in lava flow of the Squirrel Springs Canyon Andesite, looking northwest.

FIGURE 2.2. Close up of Squirrel Springs Canyon Andesite, showing large tabular plagioclase phenocrysts glistening in the sun.

FIGURE 2.4. Bulldozer cut in trough crossbedded granular sandstone near Mile 4.0.

southern margin of the granulestone-filled paleovalley. A similar outcrop pattern is found on the east side of the modern canyon. **0.3**

4.4 In trees upslope at 9:00 and 4:00, narrow ledges of Bloodgood Canyon Tuff abruptly wedge out against the underlying Squirrel Springs Canyon Andesite, a relationship that apparently defines the outer margin of the previously mentioned east-southeast-trending paleovalley filled by the granular sandstone. From here to the south for the next mile, dark gray aphanitic basaltic-andesite lavas, of the Bearwallow Mountain Andesite, unconformably overlie weathered and eroded outcrops of the Squirrel Springs Canyon Andesite. **0.5**

4.9 Culvert; road crosses tributary drainage from Antelope Tank. On the north side of this drainage, at 3:30, the basal contact of the Bearwallow Mountain Andesite (on Squirrel Springs Canyon Andesite), is approximately 40 ft above road level. On the south side of the drainage, at 10:00, basaltic Bearwallow outcrops form the modern valley floor, as much as 30 ft below road level. Similar outcrop patterns nearby indicate the road is now crossing the north wall of a late Oligocene basalt-filled paleocanyon at least 70 ft deep that was cut in the underlying Squirrel Springs Canyon Andesite. This locally east-northeast-trending paleocanyon probably merged with the previously described sandstone-filled paleovalley approximately 1 mi east of here. **0.1**

5.0 Roadcut on right in paleocanyon fill consists of dark gray olivine basalt or basaltic andesite of the Bearwallow Mountain Andesite. **0.1**

5.1 Culvert. Road crosses McKibben Tank drainage. **0.1**

5.2 Roadcut on left in Bearwallow basaltic flow, which contains a large, rounded mass of tan sandstone, possibly ripped up from the floor or walls of the underlying paleocanyon. Just beyond, road again crosses McKibben Tank drainage; here the modern valley transects the south wall of the basalt-filled paleocanyon. Approximately 40 ft of relief is visible here at the base of the Bearwallow lavas. **0.1**

5.3 Cut on right in porphyritic Squirrel Springs Canyon Andesite that defines the south margin of the paleocanyon. The Bearwallow-Squirrel Springs contact forms a break in slope 20 ft above the road at 2:00. **0.1**

5.4 Roadcut on right exposes a 10 ft zone of red clay developed on the top of the Squirrel Springs Andesite. The red clay contains angular clasts of altered andesite porphyry. This clayey zone probably represents a paleoweathering profile buried by the Bearwallow basaltic lavas at 26 Ma. Base of Bearwallow is 10 ft above road at 2:00. **0.1**

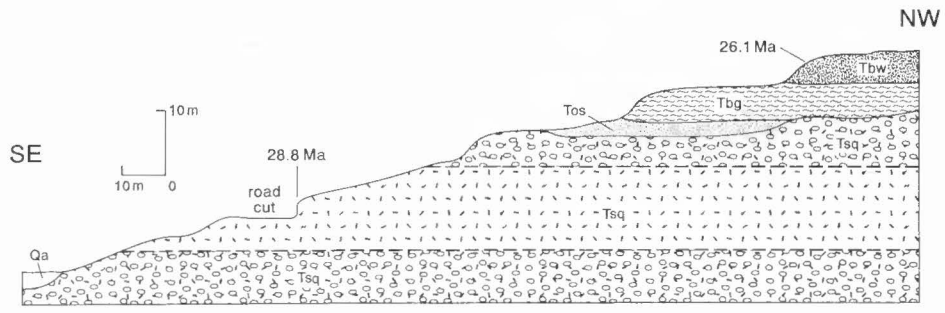

FIGURE 2.3. Sketch cross section illustrating upper Oligocene volcanic stratigraphy exposed on the west side of the western fork of El Caso Springs Canyon, Slaughter Mesa 7.5′ quadrangle. Open circle pattern in lower and upper Squirrel Springs Canyon flows represent vesicular zones. Unit abbreviations are: Tsq=Squirrel Springs Canyon Andesite; Tos=andesitic granular sandstone; Tbg=Bloodgood Canyon Tuff; Tbw=Bearwallow Mountain Andesite. Approximate locations of $^{40}Ar/^{39}Ar$ age samples are indicated.

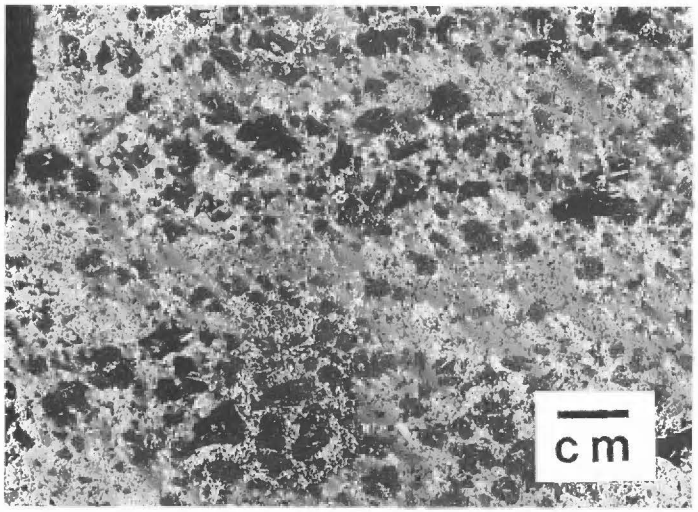

FIGURE 2.5. Close-up view of granular sandstone showing highly angular fragments of andesite porphyry in a sandy matrix.

5.5 Basal contact of Bearwallow Mountain Andesite at road level on right. **0.1**

5.6 Roadcut on right in dark gray vesicular basaltic-andesite lava containing sparse fine-grained phenocrysts of yellow-brown olivine. Bearwallow lavas are intermittently exposed for next 1.6 mi, from here to Slaughter Mesa. **1.2**

6.8 McKibben Tank is visible at valley bottom on left. **0.4**

7.2 Road crests at elevation of approximately 8690 ft. Open meadows from 12:00 to 2:00 define the shallow basin known as Slaughter Mesa. Several small borrow pits (Fig. 2.6) and local incision along upper Largo Creek Canyon indicate this open flat is underlain by 20 to 120 ft of poorly consolidated gravels derived entirely from basaltic-andesite lavas of the Bearwallow Mountain Andesite. These upper Tertiary(?) gravels are tentatively assigned to the Fence Lake Formation and appear to fill an incipient fault-block basin at the head of ancestral Largo Creek. **0.2**

7.4 From 10:30 to 1:00, a 300-ft-high Ponderosa-covered fault-line escarpment marks the trace of a Neogene normal fault that locally forms the southeast margin of the Slaughter Mesa basin. From 2:00 to 3:00 another fault-line scarp, which trends north-northwest about 200 ft above the flats, locally forms the western side of the Slaughter Mesa basin. This high-angle normal fault is well exposed 2 mi farther south, at Indio Canyon, where it displaces the Bloodgood Canyon Tuff 300 ft down to the east. Ancient colluvial breccias derived from the Bloodgood Canyon Tuff (buried by Bearwallow lavas) occur locally along the Indio Canyon fault and suggest that it may have been active as early as 28 to 26 Ma. **0.3**

7.7 Culvert, road crosses drainage of upper Largo Canyon, headwaters of the ephemeral stream that feeds Quemado Lake. **0.3**

8.0 Slow down for four-way intersection. **Continue straight ahead on FR-13**. Watch for cross traffic, most likely to be big game hunters in the early fall. The Mangas Mountains and Slaughter Mesa are a favorite area for zealous elk hunters who come great distances (Fig. 2.7) to hunt the bellowing bulls. FR-93, to right, is continuation of Slaughter Mesa loop to NM-32. Roadcuts on FR-93 approximately 8 mi from here expose 40-ft-high dune faces in the sandstone of Escondido Mountain. **0.5**

8.5 Begin ascent of Pleistocene fan surface that appears to have prograded over dissected Fence Lake gravels. **0.4**

8.9 Cattle guard. Route crosses fault-line scarp at southeast margin of Slaughter Mesa basin and enters narrow canyon of upper Largo Creek, which has cut deeply into Bearwallow Mountain Andesite on the upthrown side of the fault. **0.2**

9.1 Roadcut on left in basaltic andesite lava of Bearwallow Mountain Andesite. **0.2**

9.3 Platy cleavage resulting from flow foliation in basaltic-andesite lava is well exposed in cut on left. **0.4**

9.7 Vesicular basaltic-andesite lavas in roadcuts on left and right. **0.4**

10.1 Crest of hill. Cross "Rim Divide" of Cather et al. (this volume). **0.1**

FIGURE 2.6. View to west of borrow pit in Fence Lake Formation gravels that underlie Slaughter Mesa near intersection of FR-13 and FR-93. Tree line along west end of Slaughter Mesa delineates fault-line scarp of the Indio Canyon fault.

FIGURE 2.7. This avid hunter came a long way to "GO 4 ELK" in the Mangas Mountains.

10.2 Drill pad on left for Shell-Elf Aquitane-BP Mangas Mountains Federal Well No. 1, a wildcat well drilled in the autumn of 1987 to Precambrian basement and a total depth of 7808 ft. This is one of several hydrocarbon test wells drilled in the Mangas region during the late 1980s, as part of the "Mogollon Frontier" or "Magic Area" play (Kopacz, et al., 1989; Garmezy, 1990). General stratigraphy and some structural implications of the Mangas Mountains Federal No. 1 Well are discussed in the following minipaper. **0.3**

STRATIGRAPHIC AND STRUCTURAL IMPLICATIONS OF THE MANGAS MOUNTAINS FEDERAL NO. 1 WELL

Richard M. Chamberlin

New Mexico Bureau of Mines and Mineral Resources, Socorro, NM 87801

According to records of the New Mexico Bureau of Mines and Mineral Resources Library of Subsurface Data, the Mangus (sic, Mangas) Mountain Federal No. 1 Well intersected 4246 ft of Tertiary strata (Mogollon-Datil volcanic pile and Baca Fm.) unconformably overlying 558 ft of Triassic Chinle, unconformably overlying 2311 ft of Permian strata, unconformably overlying Precambrian basement rocks. Permian strata include 402 ft of San Andres Fm., 235 ft of Glorieta Sandstone, 1060 ft of Yeso Fm. and 614 ft of Abo Fm. In meters, the above thicknesses are 1291, 170, 703, 122, 71, 322 and 187, respectively.

The Mangas Mountains Federal No. 1 Well is collared in Bearwallow Mountain Andesite (~ 150 m thick here) at the top of the middle Tertiary volcanic pile. Thus, the total thickness of middle to early Tertiary strata, 1291 m, may be compared with the total thickness of middle to early Tertiary strata, 2137 m, estimated for the Sun Oil Co. No. 1 Well, approximately 55 km east of the Mangas Mountain well (see First-Day road log, mile 49.2). This westward decrease in thickness of about 40% probably occurs mainly within middle to late Eocene strata of the Baca Fm. and/or the lower Spears Group. Younger middle Tertiary strata (35-26 Ma) in the Sun Well (930 m) and that exposed in Mangas Mountains area (690 m, Chamberlin et al., 1994b) show a similar westward thinning trend but can only account for about 28% of the observed total thickness change (846 m). The westward thinning of middle and early Tertiary strata can be attributed to differences in relative proximity to late Eocene volcanic centers and/or relative proximity to Laramide transpressional welts (cf. Garmezy, 1990). Generally southeastward coarsening of the lower Spears group suggests the Sun Well is more proximal to an inferred late Eocene volcanic center (ca. 40-36 Ma) now buried under the southern San Agustin Plains (S. M. Cather, oral commun., 1994).

A recently published structure contour map of the base of Upper Cretaceous strata in west central New Mexico and eastern Arizona (Rauzi, 1994), including well data in the Mangas region, suggests the presence of a northwest-trending(?) Laramide syncline east of the Mangas Mountains between Alegres Mountains and Wallace Mesa. The detailed geometry of buried Laramide structures in the Mangas region is presently uncertain and may involve multiple transpressional welts along major regional structures now expressed as normal faults in the Tertiary volcanic pile (Cather, 1989; Garmezy, 1990, Chamberlin, et al., 1994b). The presence of 345 m of upper Cretaceous strata in the Sun Well (R. Foster, unpub. log, NMBMMR Subsurface Library) and the total absence of Cretaceous strata in the Mangas Mountains Federal well also implies the latter was relatively proximal to a Laramide highland. Detailed logging of cuttings (as yet not available) from the Tertiary intervals in the "Magic Play" wells could provide significant insight as to the geometry and timing of Laramide structures in the Mangas region. For a summary of Tertiary stratigraphy in the Hunt Oil Co. No. 1-16 well, approximately 23 km east of here near Wallace Mesa, see minipaper by Broadhead and Chamberlin (this road log). Broadhead (this volume) has summarized data concerning the petroleum source rock potential of pre-Tertiary rocks in the Hunt well.

10.5 Del Buey Vista. Slow down to look through breaks in tree tops at majestic view across the San Agustin depression from continental divide to continental divide (Fig. 2.8). **0.2**

10.7 Begin 400 ft descent along south-facing escarpment that locally defines the Cañon del Buey fault. This breakaway fault forms the north rim of the Sand Flat Canyon graben (see Third Day road log); it is also a scissors fault that decreases in displacement eastward to where it dies out near the north-northeast-trending Hickman fault. Topographic relief across the Cañon del Buey fault increases westerly to a maximum of 800 ft. **0.5**

11.2 At 1:00 is good view of the northeast end of the Reserve graben near Aragon. **0.1**

11.3 Sharp curve to left. Roadcuts on right and left in Bearwallow Mountain Andesite. **0.1**

11.4 For next 0.1 mi roadcuts on left provide excellent exposure of near-vent basaltic agglomerates (scoriaceous cinders and bombs) overlain by channelized flows of platy basaltic andesite lava (Fig. 2.9). Also present, below the road level on the right, are large blocks of variably oxidized (reddish orange to black) basaltic spatter that show well-developed flow structure similar to eutaxitic foliation in ash-flow tuffs (Fig. 2.10). **0.6**

12.0 Road junction on right. **Continue straight ahead on FR-13**. FR-13 crosses the continental divide here at an elevation of 8613 ft. FR-13 is now paralleling the base of the Cañon del Buey fault-line scarp; thus the continental divide crosses the road at a right angle and ascends the scarp to the ridge line at an elevation of about 9000 ft. In contrast, the continental divide ridge line south of the del Buey fault (3:00) is at an average elevation of about 8650 ft. **0.2**

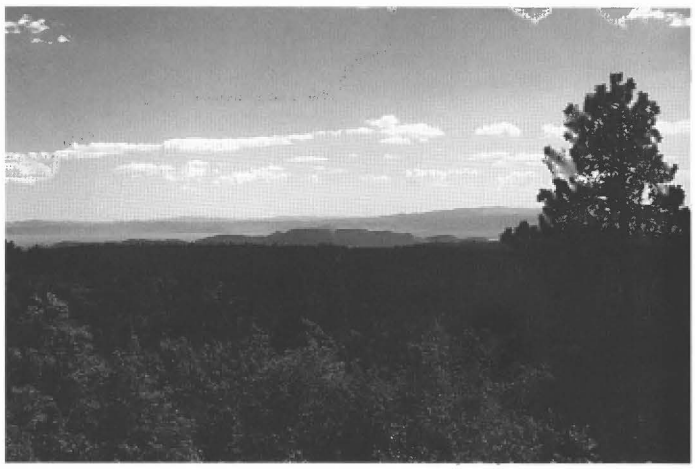

FIGURE 2.8. View to southeast across the San Agustin depression from Del Buey Vista. Ridge line in foreground is on continental divide; Cerro Caballo in low middle ground is at the west end of the San Agustin depression, and Pelona Mountain on the skyline at right is also on the continental divide. Exposures of the Horse Springs dacite at Cerro Caballo will be visited at Stop 3 on the third day of this field conference.

FIGURE 2.9. Platy to massive basaltic andesite lava fills channel cut in cinders and bombs of basaltic andesite that are interpreted as near-vent agglomerate. Road logger is standing at base of channel which rises about 16 ft to the right. Elongate vesicles at channel bottom indicate flow parallel to channel walls (S15°E).

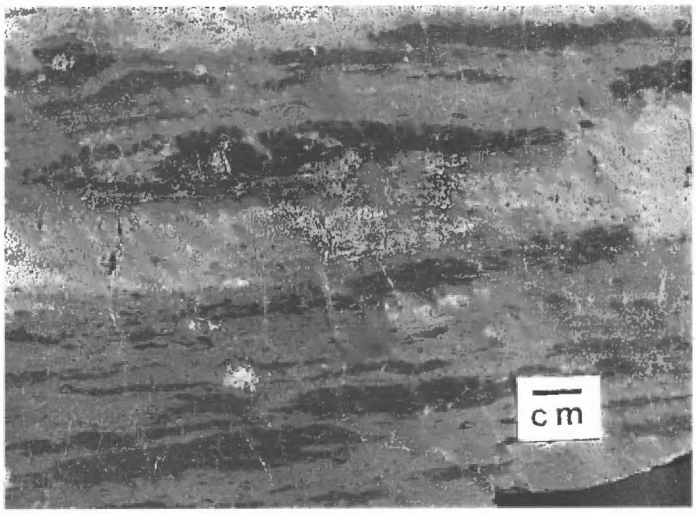

FIGURE 2.10. Flow structure developed in basaltic andesite spatter. Lighter colored matrix is dense, red and glassy. Dark streaks apparently represent unoxidized cores of lava bombs and spatter.

12.2 Steep slopes and bulldozer cuts on left in carbonate-cemented basaltic colluvium. Small blocks of white opal appear to wash out of the colluvium. Projected trace of the Cañon del Buey fault now follows the floor of Caballerzia Canyon at 3:00. **0.1**

12.3 Cut on left in massive core of basaltic-andesite lava flow. **1.4**

13.7 Dusky red vesicular top of basaltic-andesite lava flow in roadcut on left. **0.2**

13.9 Northwest flank of Mangas Mountain at 12:00 on skyline. In early autumn, look for yellow aspen groves here. **0.1**

14.0 Cross projected trace of Cañon del Buey fault where it bends north and its apparent displacement rapidly decreases to less than 100 ft. **0.6**

14.6 Descend onto older Pleistocene alluvium filling Valle Tio Vinces, a small fault-controlled depression on the downthrown western side of the north-northeast striking Hickman fault (main strand of Hickman fault zone). Surface waters exit through gap at 2:00, which is the head of Patterson Canyon. Hill slope to right of water gap (and stock tank) is underlain by Bloodgood Canyon Tuff on the upthrown side of the Hickman fault. **0.2**

14.8 Stop at intersection of FR-13 and FR-214. **Turn left on FR-214**, which leads to Mangas and US-60. Mangas Mountain, elevation 9691 ft, on skyline at 1:30. Reconnaissance mapping indicates that Mangas Mountain is underlain by as much as 1100 ft of basaltic andesite lavas, the Mangas Mountain Member of the Bearwallow Mountain Andesite. In comparison, the average thickness of Bearwallow basaltic andesite lavas in the Slaughter Mesa area is approximately 500 ft. These observations suggest the high peaks of Mangas Mountain represent the eroded apex of a basaltic-andesite shield(?) volcano of late Oligocene age (~25–26 Ma). **1.0**

15.8 Junction with FR-11 on right leads to Mangas Mountain lookout tower. **Continue straight ahead on FR-214**. Note Forest Service horse corrals on left. Water tanks at corrals are fed by a siphon from Valle Tio Vinces spring, which discharges from basaltic-andesite lava just below the tree line at 2:00. **0.5**

16.3 Cattle guard. Cross continental divide at elevation of approximately 8280 ft. Road now descends on the west side of divide following San Antone Canyon and the ephemeral drainage of Mangas Creek. Numerous cuts and canyon wall exposures in Bearwallow Mountain Andesite can be observed over next 1.9 mi. **0.4**

16.7 Sleeping Steer Tank on right. **1.5**

18.2 Basaltic andesite lava at base of Bearwallow Mountain Andesite is exposed in roadcut on left, with low roadcut just beyond in iron-stained Bloodgood Canyon Tuff. **0.2**

18.4 Canyon wall on right exposes 20 ft ledge of porphyritic Squirrel Springs Canyon Andesite overlain by 15 ft of slabby Bloodgood Canyon Tuff. **0.1**

18.5 Cut on left in Squirrel Springs lava. **0.5**

19.0 Low cut on left in dark gray flow-banded aphyric andesite of San Antone Canyon. **0.2**

19.2 Highwall (roadcut) on left in flow-banded andesite of San Antone Canyon (Fig. 2.11). A whole rock sample from this roadcut has yielded a $^{40}Ar/^{39}Ar$ isochron age of 29.2 ± 0.1 Ma (McIntosh and Chamberlin, this volume). The canyon wall on right exposes 60 ft of the andesite of San Antone Canyon, which is overlain by 10 ft of Vicks Peak Tuff and in turn by 100 ft of Squirrel Springs Canyon Andesite. This new $^{40}Ar/^{39}Ar$ age for the andesite of San Antone Canyon is in good agreement with the overlying Vicks Peak Tuff, which is well dated at 28.5 Ma. This locality may be regarded as an informal type section for this informal map unit. **0.1**

19.3 Platy base of the andesite of San Antone Canyon overlies unusually red-colored sandstone of Escondido Mountain in cut on left. **0.4**

19.7 Crossbedded sandstone of Escondido Mountain is well exposed in roadcut on left. Steepest crossbeds dip 28° to northeast. Pleistocene terrace gravels unconformably overlie the upper Oligocene sandstone here. **0.4**

20.1 Mangas Work Center on right. Reconnaissance mapping of high ridge at 1:00 to 2:30 has defined late Oligocene paleotopographic relationships similar to those observed in the west fork of El Caso Springs Canyon. These important stratigraphic relationships are well hidden by vegetation and soils (Fig. 2.12) and best illustrated in a cross section along this ridge line (Fig. 2.13). **0.1**

20.2 Large exposure of sandstone of Escondido Mountain across valley at 3:00. **0.2**

20.4 Road to Cassidera Springs on left; cattle guard beyond. **0.1**

20.5 Gallegos Ranch homestead on right. **0.2**

20.7 Cattle guard. Junction with FR-93 on left; **continue straight ahead on FR-214**. On the butte at 2:30, Bearwallow Mountain Andesite disconformably overlies the sandstone of Escondido Mountain. As illustrated in the cross section (Fig. 2.13), four regional volcanic formations are missing here. These paleotopographic relationships *may* reflect the beginning of normal fault displacement along Hickman Fault zone as early as 26 to 28 Ma. However, it is also evident that the Vicks Peak Tuff and Bloodgood Canyon Tuff fill swales between dunes in the sandstone of Escondido Mountain in the Mangas region, and that the underlying, eolian paleotopography may be the principal control on the pinch-out of these tuffs. Documenting possible growth-faults that may control the thickness of upper Oligocene volcanic units will require detailed regional mapping. **0.4**

21.1 FR-214 crosses concealed trace of a normal fault downthrown approximately 300 ft to the north; the concealed fault is a locally east-trending strand of the Hickman fault zone. **0.1**

21.2 Road bends to right and crosses Mangas Creek drainage at culvert. Road now on upper Quaternary alluvium in Mangas Creek. **0.2**

21.4 Cattle guard. Antique Gabaldon Windmill on left was operational as of autumn 1993. **0.2**

21.6 Ruins of old Gabaldon homestead in cottonwood and ash grove on left (Fig. 2.14). The building walls are slabs of fine-grained, buff colored sandstone and adobe mortar. Presumably, these slabs were quarried from a nearby outcrop of the sandstone of Escondido Mountain. **0.2**

21.8 Leaving Apache National Forest. Cattle guard. **0.2**

22.0 Pleistocene gravels underlie northeast-sloping graded surface on skyline at 9:00. **0.6**

22.6 Road-metal quarry at 3:00 was developed in low hill of Bloodgood Canyon Tuff as much as 80 ft thick. This quarry, elevation 7600 ft, lies at the structurally lowest point on the west side of the Hickman fault zone. On the northeastern corner of the Mangas Mountains, 4:00 on skyline, the Bloodgood Canyon Tuff is present on the upthrown eastern side of the Hickman zone at an elevation of 8700 ft. The apparent 1100 ft displacement is distributed on three mappable down-to-the-northwest normal faults in this 2 mi wide zone (Fig. 2.15) **0.8**

23.4 Low mesa at 8:00 consists of 300 ft of basaltic-andesite lavas of the Bearwallow Mountain Andesite overlying lenticular outcrops of Bloodgood Canyon Tuff and the sandstone of Escondido Mountain. **0.2**

23.6 Cattle guard. Stone walls of abandoned homestead at 1:00 and old schoolhouse at 12:00 are made from hand-hewn slabs of Bloodgood Canyon Tuff with an adobe mortar. On the skyline from 11:45 to 12:45, all of the low conical hills east of Mangas and the high flat-topped peaks of Alegres Mountain are capped by Bearwallow Mountain Andesite, disconformably overlying 28.5-Ma Vicks Peak Tuff and the sandstone of Escondido Mountain (Fig. 2.16). Alegres Mountain, elevation 10,229 ft, is the highest landmark on the Mogollon slope of west-central New Mexico. Alegres Mountain lies on a northeast-trending horst that defines the structurally highest block in the Mangas-Pie Town area. From Alegres Mountain to the conical hills at 11:45 the total Neogene (post 26 Ma) stratigraphic throw across the Hickman fault zone is approximately 2000 ft down to the west. As much as 500 ft of the Neogene displacement postdates the middle to upper Miocene Fence Lake Formation. **0.4**

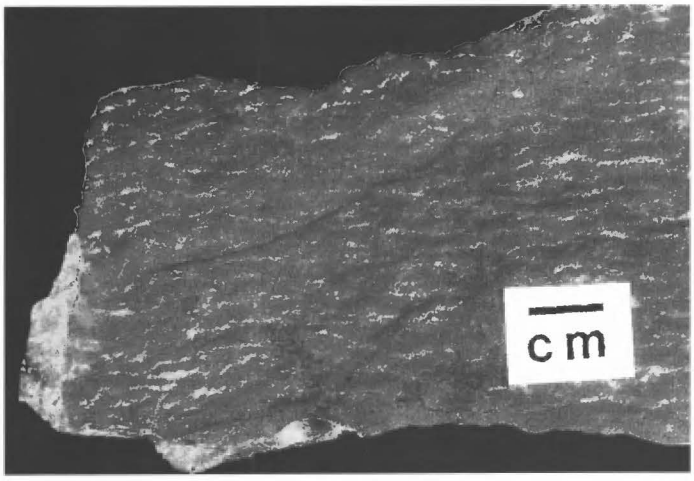

FIGURE 2.11. Close-up view showing typical discontinuous flow bands in mafic aphyric lava of the andesite of San Antone Canyon.

FIGURE 2.12. Road logger attempts binocular remote sensing to decipher Oligocene volcanic stratigraphy on ridge line east of the Mangas work center. Dark iron-strained tuffs that look like lavas from a distance and many trees make this a futile effort. Bearwallow Mountain Andesite caps butte at center and Bloodgood Canyon Tuff caps the ridge on the right.

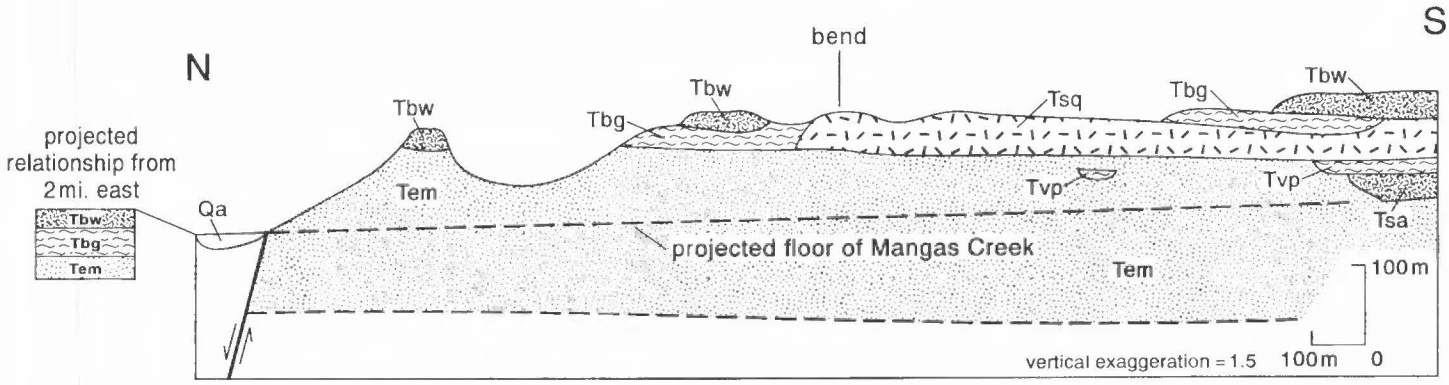

FIGURE 2.13. Cross section along ridge line east of Mangas work center. Cross section illustrates upper Oligocene volcanic stratigraphy and local unconformities that may reflect nascent (late Oligocene) fault-block topography within the Hickman fault zone. Stratigraphic relationships and present elevation of a downthrown block located 2 mi farther east (near road metal quarry) are projected to the line of section. Unit symbols: Tbw=Bearwallow Mountain Andesite, Tbg=Bloodgood Canyon Tuff, Tsq=Squirrel Springs Canyon Andesite, Tvp=Vicks Peak Tuff, Tsa=Andesite of San Antone Canyon, Tem=sandstone of Escondido Mountain.

24.0 Cross Mangas Creek to its eastern bank. For the next 14 mi, this route follows Mangas Creek valley and adjacent piedmont slopes descending from Alegres Mountain and the eastern flank of Escondido Mountain. Coarse bouldery piedmont-slope deposits on the upper rim of the broad valley are correlated with the Fence Lake Formation. Along the east rim of the valley, Fence Lake deposits are faulted and downdropped to the west. Pliocene and early to middle(?) Pleistocene alluvial fans and bajadas (Quemado Formation of Cather and McIntosh, this volume) are inset against Fence Lake Formation on both sides of the valley. The finer grained, pebbly to cobbly sands of the Quemado Formation are graded to levels 40 to 100 ft above upper Quaternary alluvium underlying the broad floodplain of Mangas Creek. **0.1**

24.1 Road rises 30 ft onto toe of middle (?) Pleistocene fan fed by Killion Canyon, which heads on the east flank of Mangas Mountain. Excellent exposures of crossbedded sandstone of Escondido Mountain and a swale-filling outcrop of 28.5-Ma Vicks Peak Tuff are present at the head of Killion Canyon (Figs. 2.17, 2.18). **0.8**

24.9 Route ascends onto Plio-Pleistocene piedmont deposits of the Quemado Formation. **0.1**

25.0 Junction, road to Greens Gap on right. **Continue straight ahead to north on county road leading to US-60** (13 mi). The Hunt No. 16-1 State Well, located about 5 mi southwest of Greens Gap, was drilled to Precambrian basement in 1987. A reevaluation of the Tertiary stratigraphy intersected in this well is presented in the following minipaper. Also see Broadhead (this volume) for a discussion of petroleum source rock potential and source rock maturity in the Hunt Well. **0.4**

FIGURE 2.14. Ruins at Gabaldon homestead.

FIGURE 2.15. View to southeast across the Hickman fault zone. High wall in left foreground is cut in Bloodgood Canyon Tuff. The northeast corner of Mangas Mountain forms a high ridge on the skyline. At north end of ridge a dark ledge of Bearwallow Mountain Andesite directly overlies the Bloodgood Canyon Tuff on the upthrown eastern side of the Hickman fault zone. The main strand of the Hickman fault parallels the base of this ridge.

FIGURE 2.16. Panorama to northeast across the Hickman fault zone from abandoned school house south of Mangas. Flat-topped peaks of Alegres Mountain on right are capped by 600 ft of Bearwallow Mountain Andesite. Conical hills beyond the schoolhouse are also capped by Bearwallow lavas at an elevation as much as 1700 ft below equivalent lavas on Alegres Mountain.

HUNT OIL CO. NO. 1-16 STATE WELL WIRELINE LOG RESPONSES, TERTIARY AND CRETACEOUS SECTIONS

Ronald F. Broadhead and Richard M. Chamberlin
New Mexico Bureau of Mines and Mineral Resources, Socorro, NM 87801

Petrographic sections of cuttings from depths of 480, 540, 750, 900, 1200, 1350, 1650, 1860, 2250, 2700, 2850, 3150, 3300 and 3600 feet in the Hunt Oil Co. No. 1-16 State well (Sec. 16, T3S, R13W) were analyzed by the junior author to evaluate lithologic breaks in the Tertiary section in this drill hole. The senior author has characterized these lithologic units in terms of their wireline log response. The results of this brief study are as follows.

The contact between plagioclase- and hornblende-rich andesitic sandstones of the lower Spears Group (formerly lower Datil Group) and quartz-rich sandstones of the Baca Formation is at 1370 ft. This contact is delineated by a sharp decrease in resistivity in the Baca as compared to the overlying Spears. This effect is seen on both the deep induction log and the spherically focused log. There is also a slight increase in radioactivity in the Baca. Scout cards for this well on file at the New Mexico Bureau of Mines and Mineral Resources petroleum records library report a pick of 510 ft depth as the top of the Baca Formation. Thin section data do not support a lithologic break at this depth.

From 1370 to 1830 ft, the Baca is characterized by uniformly low resistivity and high radioactivity and appears to be composed dominantly of shaly or muddy sediments with thin (<10 ft) sandstone/conglomerate beds. From 1830 to 2710 ft, however, the Baca consists of thickly-bedded (10-40 ft) units interbedded with the shales. These thickly-bedded units are characterized by high resistivity and low radioactivity and are most likely sandstones and conglomerates (channels?). The total thickness of *typical* Baca Formation in this hole is 1340 ft.

The interval from 2710 ft to 3290 ft may belong to a previously unrecognized pre-Baca Tertiary unit, the lowermost Baca Formation or a Tertiary zone of oxidation and weathering developed on Upper Cretaceous rocks prior to Baca deposition (Chamberlin, 1981b). Cuttings in this interval consist of uniformly red mudstones, siltstones and fine-grained sandstones. These are significantly finer grained than the overlying sediments. Compared to the overlying part of the Baca, the interval from 2710 to 3290 ft is marked by a decrease in resistivity

FIGURE 2.17. A view to north of cross bedded eolian sandstone of Escondido Mountain, which is well exposed at the head of Killion Canyon on the northeast flank of Mangas Mountain.

FIGURE 2.18. Wedge of 28.5-Ma Vicks Peak Tuff within the sandstone of Escondido Mountain at the head of Killion Canyon. The base of the unwelded tuff is banked against a late Oligocene dune face.

on both the deep induction log and the spherically focused log. Uniformly low resistivities within this part of the Tertiary are indicative of a shale/mudstone section. Thick beds of sandstones or conglomerates are conspicuous by their absence. Mottled colors typical of the pre-Baca weathering zone in outcrop (Chamberlin, 1981b) are not observed in cuttings; which places the third alternative in disfavor. The lower Baca Formation in outcrop is typically coarse grained and conglomeratic; thus the first alternative listed above might be preferred. However, the total thickness of Tertiary red beds in this well is 1920 ft, which is in good agreement with the 1830 ft of Baca Formation measured by Cather and Johnson (1984) on the north flank of the Datil Mountains. Alternatively, this lower fine-grained Tertiary unit could simply be interpreted as an unusually fine-grained basal facies of the Baca Formation.

The contact between Tertiary red beds and gray Cretaceous rocks is at 3290 ft. This contact is delineated by a marked increase in radioactivity within the organic-rich Cretaceous shales and a corresponding decrease in resistivity on both the deep induction log and the spherically focused log.

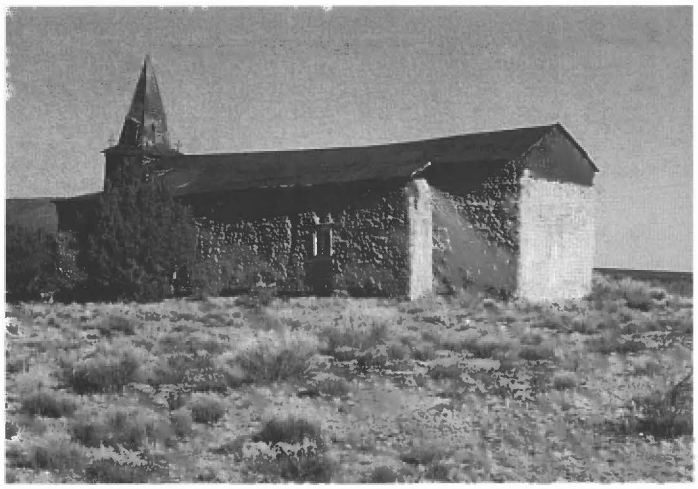

FIGURE 2.19. Abandoned church at Mangas. Bearwallow Mountain Andesite caps east flank of Escondido Mountain at skyline on left.

25.4 Entrance to Davila Ranch headquarters on right. Slow down for sharp section-corner bend in road. **0.1**

25.5 Ninety degree bend to left. **0.3**

25.8 Weather-worn adobe church at 11:00 marked the center of Mangas during the 1930s great depression era (Fig. 2.19). Mangas is Spanish for sleeve or fringe of land; and is also used in a figurative sense for "sleeves" of rain pouring from clouds in an otherwise open sky. One of the Apache chieftains who roamed this country in the mid-19th century was called Mangas Coloradas, "Red Sleeves", but it is unlikely that the place name commemorates this Apache leader. The Mangas Creek, aka Pinoville or Piñonville (?), post office was active from 1909 to 1943 (Pearce, 1965). **0.7**

26.5 Slow for sharp curve to left past cattle guard. Cross upper Quaternary floodplain of Mangas Creek for next 0.4 mi. **0.4**

26.9 Slow for sharp curve to right. For next 8.1 mi the Mangas-Omega road crosses the toes of lower to middle Quaternary alluvial fans that grade to a level about 40-60 ft above modern Mangas Creek. East of Mangas Creek, the toes of upper Pliocene to lower Pleistocene fan deposits rise 80 to 120 ft above Mangas Creek. **1.0**

27.9 Cross tributary arroyo of Mangas Creek. Good view at 3:00 of conical hills capped with Bearwallow Mountain Andesite that lie between strands of the Hickman fault zone. On northern hill, approximately 300 ft of eolian sandstone of Escondido Mountain is present between the Vicks Peak Tuff (28.5 Ma) and Caballo Blanco Tuff (31.5 Ma) (McIntosh and Chamberlin, this volume). Another 60 ft of eolian sandstone underlie the Caballo Blanco, which in turn overlies fluvial volcaniclastic conglomerates that lie above and below the 33.7-Ma Blue Canyon Tuff. **1.2**

29.1 Headquarters of McKinley ranch on right. Ranch road on left leads to upper Cañon del Macho where a large, lenticular, cliff-forming outcrop of Bloodgood Canyon Tuff as much as 100 ft thick is present within the eolian sandstone of Escondido Mountain. **0.7**

29.8 Slow down for sharp curve to left. **0.1**

29.9 Cattle guard. **0.5**

30.4 Road crests on Quemado Formation. Good view at 8:30 of cliff-forming Bloodgood Canyon Tuff in middle slope on east flank of Escondido Mountain. **0.6**

31.0 Low hill across Mangas Creek at 2:45 is capped by coarse Fence Lake gravels. Just north of this hill another isolated Fence Lake outcrop unconformably overlies pumiceous sandstones correlative with the upper Eocene (34-35 Ma) volcaniclastic unit of Cañon del Leon (Chamberlin and Harris, this volume). This bedrock exposure demonstrates that the alluvial fill of the Mangas Valley is locally not more than 100 ft thick. Road crosses projected trace of concealed northeast-trending normal fault (down to northwest) near here. From here northward, the thin Plio-Pleistocene fill of the Mangas Valley grades into the thicker (as much as 600 ft) middle Miocene to Pleistocene fill of the structural depression referred to here as the Omega Basin syncline. **1.0**

32.0 Escondido Mountain at 9:30 (Fig. 2.20). Note decreasing northward slope (primary dip) on upper surface of Fence Lake Formation at 10:00. **0.5**

32.5 Cuestas on skyline from 11:30 to 1:30, capped with Fence Lake Formation, slope gently away from each other and appear to outline the crest of a breached anticline of Pliocene or Pleistocene age (Fig. 2.21). Grassy hills underlain by Pliocene-Pleistocene alluvium (Quemado Formation) in the middle foreground are inset against piñon-juniper-covered Fence Lake deposits on the sky line. **0.2**

32.7 Snakeweed herbicide spray test area of Quemado Soil Conservation District on right. **1.8**

34.5 Old adobe homestead at 2:00. Nearby stock well probably taps an unconfined aquifer within Plio-Pleistocene alluvium or possibly the underlying Fence Lake Formation. These permeable units most likely rest unconformably on andesitic sandstones of the lower Spears Group, which tend to act as an aquitard. Estimated thickness of alluvial fill here is 200-300 ft.

FIGURE 2.20 View southwest toward Escondido Mountain (peak on right). Snow outlines dual cliff-forming flows of Squirrel Springs Canyon Andesite overlain by Bearwallow Mountain Andesite. Bearwallow is much thicker on Escondido Mountain, but reconnaissance shows no clear indication of a vent here.

FIGURE 2.22. View across the Omega Basin eastward to the Datil-Sawtooth Mountains on the skyline. Note gentle southward dip slope defined by the crest of the Datil Mountains.

Datil Mountains on skyline at 3:00 to 4:00 form a broad south-sloping cuesta and locally define the gentle south dip of the Mogollon slope (Fig. 2.22). **1.0**

35.5 Ascend hill of Plio-Pleistocene alluvium (Quemado Formation) on northeast side of Mangas Creek valley. Roadcuts in buff-colored carbonate-cemented sandstone and gravels–typical Plio-Pleistocene alluvial deposits. **1.1**

36.6 Road continues to traverse broad plain underlain by Plio-Pleistocene alluvial sands and silts of the Quemado Formation. These deposits accumulated in the Omega Basin, the easternmost of several paleovalley/basin systems in western New Mexico that are incised into Fence Lake and older strata in the upper reaches of tributaries to the ancestral Little Colorado River. The deposits in the westernmost basin (Cow Springs Basin; see below) are Pliocene and are demonstrably correlative with the upper part of the Bidahochi Formation. However, some of the alluvium in the Red Hill basin to the east is Pleistocene (McIntosh and Cather, this volume) and thus postdates the end of Bidahochi deposition in Arizona. The Omega basin differs from basins to the west in that it is partly of structural origin due to subsidence along the Hickman fault zone that bounds the basin on the east. The western basins appear to be largely erosional in origin. **1.6**

FIGURE 2.21. View to north across Omega Basin to area southwest of Adams Diggings, where cuestas capped by Fence Lake Formation appear to define a breached anticline.

38.2 Stop Sign, Junction with US-60. **Turn left onto US-60**. **1.1**

39.3 Milepost 42 at Omega (pronounced Omeega) Village limit. **0.1**

39.4 Road to Adams Diggings on right. **1.0**

40.4 Low roadcuts on right and left in sandy Quemado Formation alluvium, locally inset against the Fence Lake Formation. **0.3**

40.7 Road rises onto moderately indurated conglomeratic sandstones and gravels of the Fence Lake Formation, which are well exposed in roadcuts for next 0.2 mi. **0.5**

41.2 **STOP 1.** Slow and park along right side of highway, as directed by flag persons. Walk past borrow pit at 1:00 to top of hill for discussion of petroleum exploration wells in the Mangas-Alegres Mountain area (see Fig. 2.23 for orientation of landmarks), regional seismic reflection profiles (minipaper by Armstrong and Chamberlin, First Day road log), and the geology and hydrology of the Largo Creek drainage basin (minipaper by Newcomer, below). Borrow pit is on BLM land, but adjacent land is private property. Later, walk to roadcuts just west of here on Highway 60 and examine the base of the Fence Lake Formation (Fig. 2.24), where it rests unconformably on the lower Spears Group (Fig. 2.25). These gray sandstones and pale red mudstones are assigned to the volcanclastic unit of Largo Creek of the Spears Group (Chamberlin and Harris, this volume). **0.2**

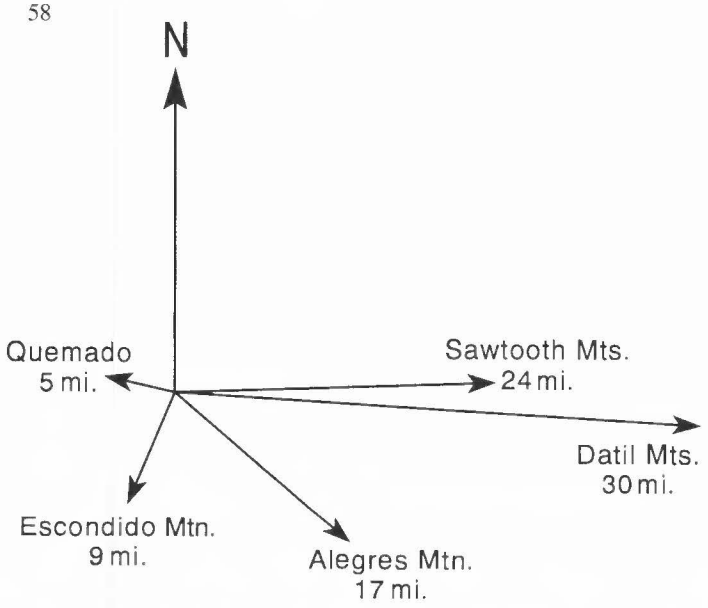

FIGURE 2.23. Panoramic index at Stop 1.

FIGURE 2.24. Basalt cobble conglomerate of basal Fence Lake Formation (upper Miocene) unconformably overlying argillaceous andesitic sandstones of the volcaniclastic unit of Largo Creek, of the lower Spears Group. Cobble imbrication suggests northwesterly paleoflow (right to left). View to east along US-60.

FIGURE 2.25. Angular unconformity consisting of horizontal Fence Lake conglomerate (upper Miocene) and associated cap of laminar calcrete overlying moderately west-tilted argillaceous andesitic sandstones and siltstones of the lower Spears Group. Small down-to-the-east normal faults cut the lower Spears Group but not the overlying Fence Lake Formation. Known regional fault zones do not project into this area; thus the significance of this pre-Fence Lake deformation is uncertain. Lower Spears Group beds are also folded and thrust faulted approximately 10 mi south of Quemado along NM-32 (see First Day road log). That deformation may be late Laramide (ca. 36-39 Ma).

HYDROGEOLOGY AND GROUND-WATER QUALITY, LARGO CREEK BASIN, CATRON COUNTY, NEW MEXICO

Robert W. Newcomer, Jr.

John Shomaker & Associates, Inc., Albuquerque, NM 87107

The Largo Creek basin is a somewhat circular drainage basin, which includes the Omega structural basin. The drainage area (Fig. 2.26) is about 660 mi^2. Its boundaries include the Continental Divide along the eastern and southern sides; the drainage divide separating Agua Fria and Largo Creeks on the west; and the drainage divide separating Frenchs Arroyo and Largo Creek on the north. Elevations range from about 10,200 to 6700 ft; the highest points are along the eastern and southern edges of the basin.

The major drainage in the basin is Largo Creek, with Rito, Escondido, San Ignacio and Mangas Creeks as tributaries. Surface water flow from the basin is to the northwest in Largo Creek. Shallow ground-water flow directions mimic surface-water flow directions, generally to the west-northwest, tributary to the Little Colorado drainage system.

Annual precipitation at Quemado and Pie Town is 15 and 9.5 in., respectively; the wettest months are during the "monsoon season" in July, August and September (Gabin and Lesperance, 1976). Precipitation is greater at higher elevations in the basin. The average annual precipitation at measuring stations above 8000 ft at several places in Catron County was greater than 21 in.

The Largo Creek basin has not been recognized by the State Engineer, who has responsibility for the supervision of the State's water resources. His jurisdiction over the State's surface water includes ground water in declared ground-water basins. A ground-water basin is generally declared when rapid development of the area might impair existing rights (Harris, 1984). The State Engineer, therefore, would have no jurisdiction concerning the use of ground water in the Largo Creek basin, except to prevent waste. The principal uses of ground and surface waters in the area are livestock watering, domestic supply and some irrigation.

The Largo Creek drainage basin includes the Omega structural basin, which consists of a down-dropped block within and west of the Hickman fault zone. The Hickman fault zone has experienced Laramide, right lateral reverse fault movement and younger Neogene normal movement (Chamberlin et al., 1994). The Eocene Baca Formation and Eocene to Oligocene volcanic and volcaniclastic rocks crop out within the drainage basin.

Little is known of the hydrogeology of the basin area. Myers (1992) described the hydrogeology of San Agustin Coal Area and the area southeast of it, which includes the northern part of the Largo Creek basin. Stone (this volume) summarized the hydrogeology of the Nations Draw area, in the San Agustin Coal Area. These areas have been studied primarily due to active exploration and development of coal resources.

The Fence Lake Formation unconformably overlies the Baca Formation in the northwestern part of the basin and overlies the Spears Group volcaniclastic rocks in the central and southern part of the Largo Creek basin. Spears Group volcaniclastic rocks were formerly assigned to the Datil Group; see Cather et al. (this volume) for revisions to Tertiary stratigraphic nomenclature in western New Mexico.

The Fence Lake Formation is a fluvial boulder to cobble conglomerate with gravelly sandstone in the upper part. The clasts are dominantly upper Oligocene basalt plus sparse Oligocene tuff and Eocene dacitic sandstones derived from the lower Spears Group near Pie Town (Chamberlin et al., 1994).

The aquifers in the Largo Creek basin are in permeable units of the Baca Formation, Spears Group and the lower part of the Fence Lake Formation. Depths to water in wells completed in these units range from within a few feet of the surface, along Rito and Largo Creeks, to greater than 200 ft at higher elevations between drainages. Quaternary alluvial fill may contain water locally, along the bottoms of major

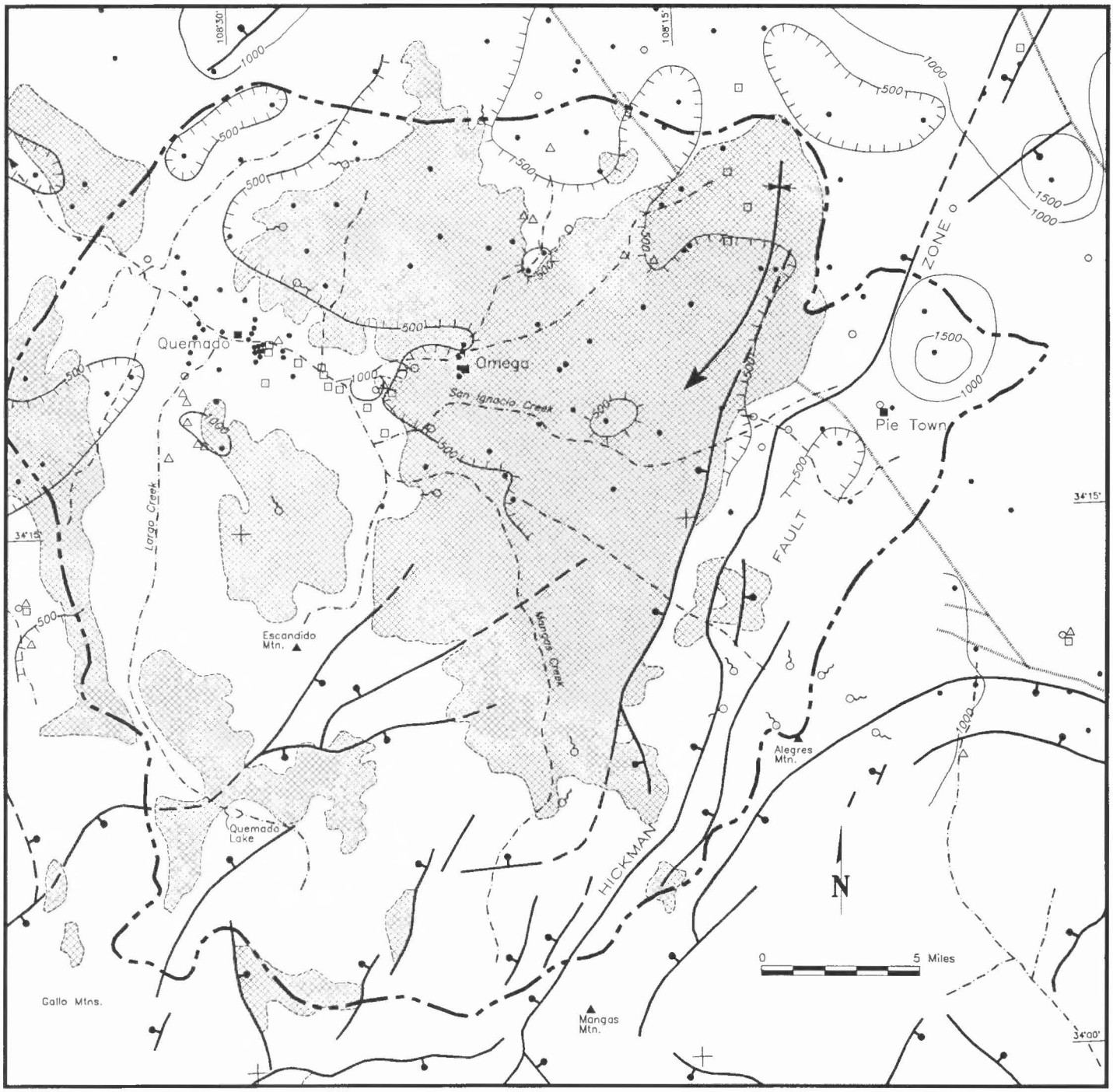

Legend

- Topographic Edge of Basin
- Perenial or Ephemeral Drainage
- Miocene: Mastly Fence Lake Formation; Includes Inset Pliacine Alluvium SE of Omega
- 500 Conductivity Contour (μmhos/cm) (hachured on low side)
- Fault (symbol on down side) (dashed where inferred)
- Basaltic Dike
- ■ Village
- Spring
- • Sample Point (well, spring, or surface water)
- ○ U >20 (ppb)
- □ As >50 (ppb)
- △ Se >50 (ppb)

FIGURE 2.26. Map of the Largo Creek drainage basin showing geologic structure, outcrop of the Fence Lake Formation, water-sample points and water-quality data. Geology is modified after Chamberlin et al. (1994); water-quality data is from Morgan (1980).

drainages; water levels probably fluctuate seasonally in response to precipitation events and snow melt. Deeper rocks may yield ground water to wells, but the drilling depths would be excessive, and the water quality is likely to be poor.

The Fence Lake Formation and Quaternary alluvium appear to be the most important aquifers. The saturated thickness of these units vary from 0 to greater than 200 ft, and are significant in the synclinal structure west of the Hickman Fault zone, and in a down-dropped fault block near Quemado Lake (Fig. 2.26). In most other areas, the Fence Lake Formation is above the regional water table.

The shallow aquifers in the Fence Lake Formation and Spears Group appear to be recharged primarily by infiltration through the overlying soils and Quaternary alluvium. Some recharge occurs directly to these units where they crop out. As shown in Myers (1992, fig. 9), water-level contours of the potentiometric surface of the aquifer in the Datil Group (now Spears Group) indicate an area of recharge about 10 mi northeast of Quemado. The "Datil Group" aquifer of Myers probably includes unrecognized saturated zones in the Fence Lake Formation, east of Omega. Other major areas of recharge are near the eastern and southern margins of the basin, in areas that receive greater amounts of precipitation.

Ground-water flow in the aquifer(s) in the Baca Formation, Spears Group, Fence Lake Formation and Quaternary alluvium is generally to the west and northwest, parallel to the surface drainages (Myers, 1992). Discharge from the Fence Lake Formation and Quaternary alluvium is evident as springs, which are typically near or above the contact with the underlying Baca Formation and Spears Group. This suggests that these rocks are less permeable than overlying Fence Lake strata and the younger alluvium. The steepening of contours of water levels in the Baca Formation, west of Quemado, reflect a lower hydraulic conductivity of these rocks.

The nature of ground-water quality in the Largo Creek basin was inferred from a study by Morgan (1980), which involved a detailed geochemical survey of well waters in the area as part of a hydrogeochemical and stream-sediment sampling program to evaluate potential uranium resources. Several hundred water samples were collected from wells in the Quemado area and analyzed for uranium and 23 other elements, together with alkalinity.

Ground water in the Fence Lake Formation in the northern half of the basin mostly has chemical conductivities less than 500 micromhos/cm. According to analyses in Myers (1992), the ground water is a sodium-bicarbonate type. Water-quality data was lacking for the southern half of the basin. Ground water from underlying Spears Group and Baca Formation, for the most part, had higher conductivities, 500 to more than 1,000 micromhos/cm (Fig. 2.26).

Elevated levels of uranium were measured in some the ground-water samples from the Baca Formation, particularly in the vicinity of the Hickman Fault zone near Pietown (Fig 2.26). According to Morgan (1980), uranium concentrations in ground water ranged from less than 0.02 to 133 ppb.

The elevated arsenic and selenium concentrations in ground water appear to be associated with volcaniclastic rocks of the lower Spears Group. Arsenic concentrations range from less than 43 to 169 ppb, and selenium concentrations range from less than 47 to 108 ppb. The lower values of the two ranges were the reported detection limits for the analyses.

The distribution of elevated concentrations of arsenic, selenium and uranium in ground waters corresponds to the areal distribution of geologic units. Arsenic and selenium are associated with andesitic sandstones in the lower Spears Group (R. M. Chamberlin, personal commun., 1994). Uranium concentrations coincide with the Baca Formation, which is known to contain uranium mineralization in the Datil Mountains region (Chamberlin, 1981).

41.4 Milepost 40. Begin descent of steep grade into valley of Rito Creek and Escondido Creek. Roadcut ahead on right exposes Fence Lake Formation unconformably overlying upper Eocene sandstones and mudstones of the volcaniclastic unit of Largo Creek. **1.2**

42.6 Road on upper Quaternary fill of Escondido Creek valley. Roadcut on left exposes older axial stream deposits (Quemado Formation, upper Pliocene to lower Pleistocene?), unconformably deposited on upper Eocene volcaniclastic unit of Largo Creek. **0.7**

43.3 Cuts on right and left in light gray andesitic sandstones and pale red mudstones of the volcaniclastic unit of Largo Creek, the lowest stratigraphic unit of the Spears Group in the Quemado region. **0.3**

43.6 Roadcut on left in tan, well-sorted pebbly sand deposited by an axial stream of late Pliocene to early Pleistocene age. Elongate hills capped by reworked Fence Lake gravels on both flanks of Rito Creek Valley are interpreted as high-energy arroyo fills graded to a late Pliocene or Pleistocene axial stream 60 to 80 feet above the road level. **0.2**

43.8 Round knob on right exposes mudstones and andesitic sandstones of the volcaniclastic unit of Largo Creek. **1.0**

44.8 Cut on left in 20 ft of weakly indurated light brown sandstones and conglomeratic sandstones of Quemado Formation. Pebble imbrications indicate westerly paleoflow of ancestral Rito Creek in the finer beds. Cobble imbrications in basal bed indicate northerly flow, presumably in a tributary arroyo. These alluvial deposits are probably late Pliocene to early Pleistocene in age. This roadcut is a reference area for the Quemado Formation (Cather and McIntosh, this volume). **0.5**

45.3 Cliffs of lower Spears Group capped by Fence Lake Formation 9:00 to 10:00. **1.3**

46.6 Roadcuts on right in buff coarse-grained sandstones and red mudstones of the upper Baca Formation (middle to upper Eocene). **0.2**

46.8 Junction, NM-36 to Fence Lake on right. **Continue straight ahead on US-60. 0.1**

46.9 Quemado Post Office on left. Quemado (Spanish, "burned") is a ranching community established about 1880 by Jose Antonio Padilla and his family, of Belen (Pearce, 1965). **0.6**

47.5 Junction with NM-32 on left. **Continue west on US-60. 0.1**

47.6 Crossing Largo Creek. Upper Quaternary alluvium forms broad, weakly dissected floor to valley. **1.0**

48.6 Junction, US-60 and NM-601. **Turn north on NM-601. 0.1**

48.7 Mariano Mesa (1:00 to 2:00) consists of Baca Formation disconformably overlain by Fence Lake Formation. The Fence Lake is 200 ft thick on Mariano Mesa (Guilinger, 1982). Flat-top mesa to south beyond Quemado is capped by Fence Lake Formation overlying volcaniclastic sandstone of lower Spears Group (Fig. 2.27). **0.7**

49.4 Tejana Mesa (11:30 -12:30) consists of capping upper Miocene basaltic lavas underlain by Fence Lake, Baca and Moreno Hill Formations. **0.8**

50.2 Pavement ends. Red and gray strata on hill at 3:00 are Baca Formation. **0.6**

50.8 Red hills at 10:00 to 12:00 are Baca Formation. Mesas on skyline 10:30 to 11:30 are capped by upper Miocene basalts that overlie Fence Lake Formation,

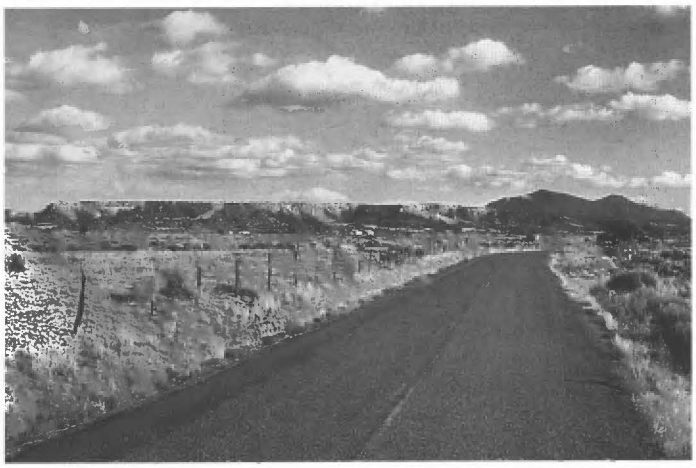

FIGURE 2.27. View south toward Quemado. Mesa on skyline is capped by Fence Lake Formation (middle-upper Miocene), which overlies upper Eocene volcaniclastic unit of Largo Creek.

which, in turn, overlies Baca Formation. Watergap at El Porticito ahead at 12:00. **0.8**

51.6 North-trending fault parallels road and juxtaposes pinkish-gray Baca sandstones against green and gray shales of Upper Cretaceous Moreno Hill Formation in roadcut on left. Conglomeratic deposits on north and south ends of roadcut are inset Plio-Pleistocene(?) fluvial deposits consisting largely of recycled Baca clasts. **0.9**

52.5 Baca Formation in roadcuts. **0.1**

52.6 Crossing arroyo that drains Amen Canyon. **0.2**

52.8 El Porticito fissure vent at 12:00. Note dramatic thickening of lava flows on Tejana Mesa toward fissure vent (Fig. 2.28). A recently obtained $^{40}Ar/^{39}Ar$ age for intrusive rocks at the El Porticito vent (7.92 ± 0.20 Ma; McIntosh and Cather, this volume) is somewhat older than the age obtained for a lava exposed near the south end of Tejana Mesa (6.73 ± 0.18 Ma; Dethier et al., 1986). El Porticito is one of nearly a dozen vents developed along a northeast-trending fault zone that can be traced for at least 25 mi.

53.2 **STOP 2.** Park along right side of road and walk to fissure vent at 1:00 to discuss the late Cenozoic volcanology and petrology of the Quemado area (see minipaper by Baldridge), soil development on Tejana Mesa (see minipaper by Love et al.), and a planned coal mine nearby to the northeast (see minipaper by Anderson). **Retrace route to US-60. 4.6**

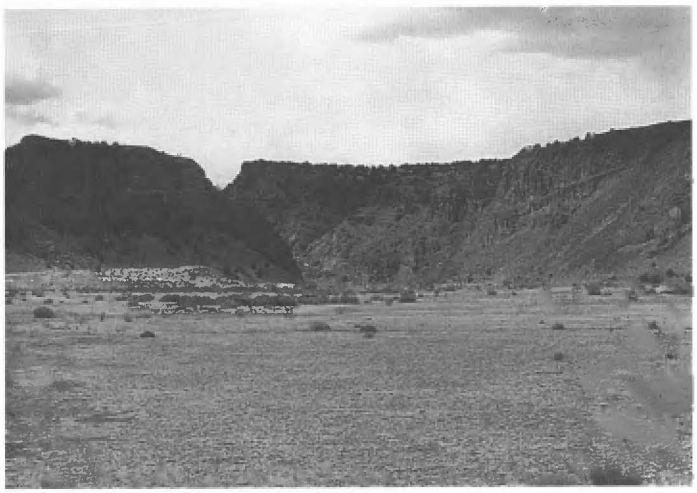

FIGURE 2.28. View north toward El Porticito fissure vent (left) and Tejana Mesa (right). Note thickening of lavas visible on escarpment of Tejana Mesa.

PETROLOGIC SUMMARY OF LATE MIOCENE VOLCANIC ROCKS OF EL PORTICITO

W. S. Baldridge

Earth and Space Sciences Division, Los Alamos National Laboratory, Los Alamos, NM 87545

The lava exposed on the southeastern face of El Porticito, as well as the lowermost flow on the southern end of Tejana Mesa, exhibits numerous light-colored sill- and dike-like structures ranging in size from several centimeters to over five meters in thickness (Guilinger, 1982; Baldridge et al., 1989). The host rock contains phenocrysts of olivine and titanaugite in a holocrystalline groundmass of clinopyroxene, sanidine, and nepheline(?). Based on its mineralogy, which includes no identifiable plagioclase, the rock appears to be phonolite. The sill- and dike-like structures, which appear to be intrusions into or segregations from the host rock, are composed of coarse-grained nepheline syenite, characterized by abundant centimeter-sized clinopyroxene grains surrounded by nepheline crystals, all characterized by bostonitic texture, in which K-feldspar forms irregular interlocking laths, as well as by a poikilitic texture. The host and sill/dike rocks appear to be of similar mineralogical composition. The host rock has been dated at 7.92 ± 0.20 Ma (McIntosh and Cather, this volume).

The unusual sill- and dike-like features exposed here may have been produced as segregations directly from the enclosing host magmas, or by intrusion into the (partially molten?) host of melts from a separate, deeper magma source. If the coarse-grained nepheline syenite represents segregation of an evolved melt fraction produced by in situ differentiation, then the minerals of these segregations would be similar to but compositionally more evolved than the minerals of the host melts. The bulk composition of the syenite would be much more enriched in incompatible elements than the host. In contrast, if the syenitic structures were emplaced into the host by intrusion from below, they could simply represent the coarser-grained crystallization products of a similar (or the same) magma. Either possibility could suggest that the sill- and dike-like structures reflect the dynamic processes within a lava lake. Since, at present, data are not available to determine the exact origin of these unusual petrological features, further detailed work is required.

SOIL DEVELOPMENT WITHIN AND AT THE TOP OF THE FENCE LAKE FORMATION AT TEJANA MESA

David W. Love[1], Bruce Harrison[2] and John W. Hawley[1]

[1]New Mexico Bureau of Mines and Mineral Resources, Socorro, NM 87801; [2]Geoscience Department, New Mexico Institute of Mining and Technology, Socorro, NM 87801

The purpose of this minipaper is to call attention to some unusual soils within the Fence Lake Formation exposed on the southwest side of Tejana Mesa, with the hope that further study will follow. The Fence Lake Formation (Miocene, Barstovian and younger, Lucas and Anderson, this volume) consists of conglomeratic and sandstone units and at least one petrocalcic horizon in its designated but yet-to-be-measured-and-described type section (McLellan et al., 1982; J. Hawley, unpubl.). In exposures of the uppermost Fence Lake Formation near Quemado and at Moreno Hill, an impressive, typical stage VI petrocalcic zone (Btkm and Bkm horizons in soil nomenclature; see Hawley, 1993, for summary) caps the local mesas. The overlying horizons (such as Bw, Bt and Av horizons) appear to overlie the well-developed

petrocalcic and may be of much more recent origin than the Btkm horizon. The Btkm horizon at these localities generally is light gray to creamy white (10 YR 8/1).

The soil exposures on Tejana Mesa are just northwest of El Porticito vent. They are preserved magnificently by burial beneath base-surge deposits and 6.7 Ma (Dethier et al., 1986) basalt flows that cap the mesa. The Fence Lake Formation at this locality is about 20 m thick with at least 2 m of relief at its base where cobble-bearing gravelly channels scoured into the underlying upper Baca Formation. The soils near the top of the Fence Lake Formation exhibit peculiarities in color, texture and structure (and probably mineralogy) that indicate different circumstances affected soil development here (Figure 2.29). Beneath the base surge deposits, the top of the Fence Lake Formation is described as follows:

0-4.5 cm	Av horizon; baked red (Munsell color 5 YR 5/4) prismatic sand and silt with mudcracks filled by base surge ash; small crystals (calcite?) partially fill vesicles.
4.5-12.5	Bk1 horizon; similar red, pebbly sand with 8-cm long, 2-cm wide, vertical calcium carbonate nodules.
12.5-19	Bk2 orange (reddish yellow 7.5 YR 7/6) pebbly sand.
19-35	K1 (Stage III); similar orange sand with large (to 4 cm wide), white, vertical, calcium carbonate nodules that grade down into krotovina with concave-up carbonate menisci marking burrow slumps.
35-50	Bk3 horizon; carbonate-bearing krotovina continue downward in orange pebbly sand.
50-75	K2 (Stage IV); degraded, hard, brecciated, calcium carbonate clasts and carbonate-cemented krotovina in orange sandy matrix.
75-95	K3 (Stage V); cross-cutting unit beneath; hard, brecciated clasts of calcium carbonate in "fine earth", soft, granular carbonate matrix; vestiges of underlying pipe-margin structure penetrates upward to 80 cm; white zone of K fabric continues in massive pebbly sand across top of underlying soil pipe in typical late stage III carbonate morphology.
85-100	K4; hard, brecciated clasts of calcium carbonate cut by overlying unit and by underlying vertical pipe-margin structure.
100-120(?)	K5; massive, faintly laminar gray calcium carbonate; vertical pipe-margin laminar structure better preserved.
120-200	K5; structureless, less carbonate cemented, tan, pebbly sand; soil pipes overhung and appear to connect below 200 cm.

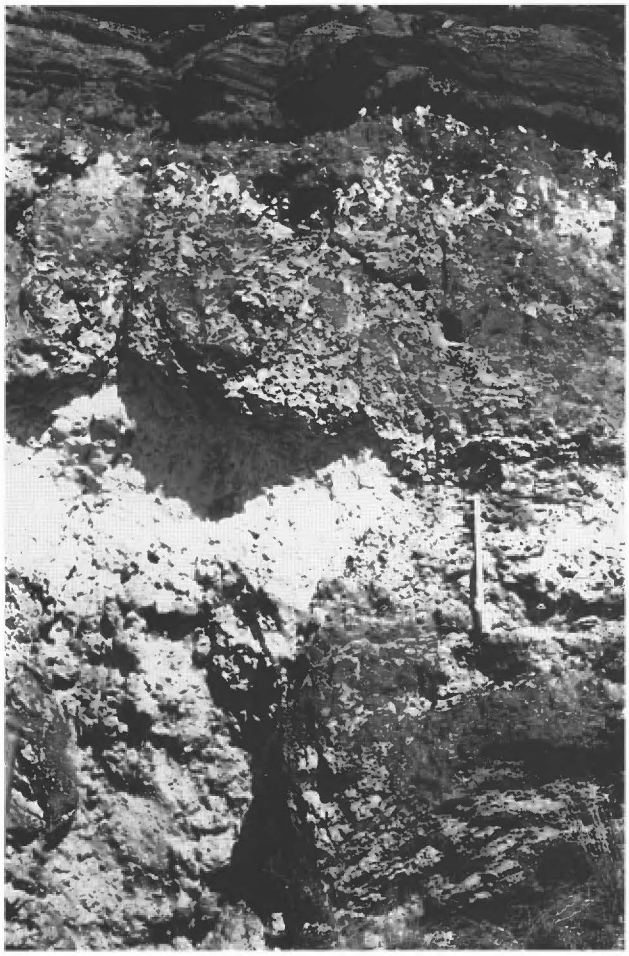

FIGURE 2.29. Soil development in uppermost 6 ft of Fence Lake Formation near Porticito. Base-surge deposits cover soil at top of photograph. Stage III calcium carbonate accumulation at level of tape measure degrades older Stage V Btkm horizon and plugs older soil pipe formed in lower horizon.

Below 200 to 400 cm are three stacked, somewhat corroded, gray, laminar (Stage IV-V) Bkm horizons with well churned, weakly carbonate-cemented, tan, pebbly sand beneath each Bkm horizon. Below 300 cm to the top of the basal gravelly channels are multiple (at least 15) intervals of massive (well churned) tan pebbly sand with variable amounts of carbonate impregnation. These structureless units commonly cap cross-bedded sandy gravels or coarse gravel channels. At least four of the massive intervals have indistinct or incipient soil pipes ranging to 2 m in vertical dimension.

At 5.5 m below the top of the Fence Lake Formation is an extremely well indurated ledge of medium gray carbonate- (and silica-?) cemented sandstone that displays micro-laminations in the upper part. On closer inspection, however, the laminations are small concentrations of manganese and silica(?) and are not the typical pedogenic laminations seen in the upper soils. Manganese staining also coats pebbles in the gravelly units.

The complex calcium-carbonate horizons below 20 cm indicate multiple episodes of carbonate accumulation. The K1 and Bk1 horizons contain carbonate nodules that have the morphology of krotovinas, similar to those described by McDonald and Busacca (1990) for carbonate nodules forming around cicada burrows in the Palouse loess. The stacked sequence of carbonate horizons could represent either an aggrading soil profile with the carbonate horizons developing during hiatuses in the depositional record, or climatic change with increasingly more arid conditions resulting in carbonate precipitation closer to the surface through time. The thick, indurated unit below 100 cm is a well-developed Stage V petrocalcic horizon (Btkm and Bkm), complete with laminated vertical pipes, but it is degraded at the top and grayer than similar horizons elsewhere in New Mexico. The laminar-carbonate-coated pipes are reminiscent of features illustrated by Gile et al. (1981, figs. 37 and 38). However, genetic pathways producing these features at Tejana Mesa are probably more complex and reflect an age three to six times older. The degradation (brecciation, invasion of fine-grained carbonate) appears to have taken place when a stage IV carbonate accumulated in the interval from 50 to 100 cm and plugged the previously formed soil pipe.

Several lines of evidence point to at least episodic water saturation and enhanced Fe, Mn and $CaCO_3$ mobility and precipitation in the uppermost Fence Lake Formation and overlying base-surge deposits: (1) cementation and red-purple color changes upward within the base-surge deposits, (2) presence of small calcite(?) crystals in vesicles in the Av horizon and calcium carbonate nodules within 5 cm of the former surface, and (3) manganese staining in most laminar horizons and gravel units at depth. The odd colors within the base-surge deposits and particularly in the Av horizon may indicate heat as well as water (steam?) altered the iron oxides within these units.

UPPER CRETACEOUS ROCKS OF THE TEJANA MESA AREA AND THE SALT LAKE COAL FIELD

Orin J. Anderson

New Mexico Bureau of Mines and Mineral Resources, Socorro, NM 87801

Upper Cretaceous rocks exposed in the low areas surrounding Tejana Mesa are the upper part of the Moreno Hill Formation. Named by McLellan et. al. (1983) for exposures at Moreno Hill, some 14 mi northwest of here, The Moreno Hill Formation is a non-marine, coal-bearing unit that approaches 600 ft in thickness. Outcrops of the formation define the Salt Lake coal field. Sandstone and shale (or mudstone) predominate. The sandstone is generally fine grained, crossbedded, grayish orange and quartzose, although facies have been described as feldspathic litharenite or arkosic (Johansen, 1986). The mudstones, which predominate locally, consist of gray or dusky yellow to dark gray, carbonaceous facies up to 100 ft in thickness. The mudstone or shale intervals are, however, interspersed with thin siltstone or very fine-grained sandstone. Coal constitutes a mere 2 to 3% of the section, but it is low-sulfur (< 1% S) and in beds of minable thickness (see Rodgers, this volume).

Depositional environments represented by the Moreno Hill Formation are fluvial channel sandstone, and associated extensive floodplain deposits in a lower coastal plain setting. The sequence was deposited on a sandstone platform, the Atarque Sandstone, that prograded out into the Mancos seaway during middle Turonian time. Based on stratigraphic position and geometry (Fig. 2.30), the coal beds represent accumulation in paralic peat swamps.

The regression that initiated this sequence was limited to the New Mexico area of the Western Interior seaway. It was probably not associated with eustatic change in sea level. It is pre-Ferron Sandstone (Utah) and demonstrably pre-Gallup Sandstone, on the basis of molluscan fauna and stratigraphic position. Both the Ferron and Gallup (late Turonian-early Coniacian) have been related to eustatic fall of sea level and to renewed activity in the Sevier overthrust belt in Utah.

The Atarque-Moreno Hill sequence, and the partly equivalent Tres Hermanos Formation in a more seaward (northeast) direction, probably represent a response to a major climatic change in the southwestern part of the continent. The climate perhaps became much more maritime and humid with the encroachment from the east of the Western Interior seaway; maximum extent of the seaway occurred during the Greenhorn cycle of sedimentation when the shoreline coincided with a line from southwestern Utah to southwestern New Mexico. Temporally this occurred at the Cenomanian-Turonian boundary. The climatic impact of this transgression was extreme and the fluvial response resulted in the progradation of a lower coastal plain environment out into the Mancos Seaway. The process was self-limiting in the sense that withdrawal of the sea allowed the return of a more moderate climate in the source area, with an attendant decrease in runoff and sediment transport. This in turn was reflected in an interruption in sediment supply to the shoreline, and progradation ceased. Lithostratigraphic expression of this progradational event (shoreline regression) is recognized as far eastward as the Sierra Blanca-Capitan area in central to southeastern New Mexico. Further evidence of the interruption in clastic supply at this time is the presence of a calcareous interval in the Mancos Shale, called the Juana Lopez Member, in a stratigraphic position correlative with subsequent (late Middle Turonian) shoreline transgression.

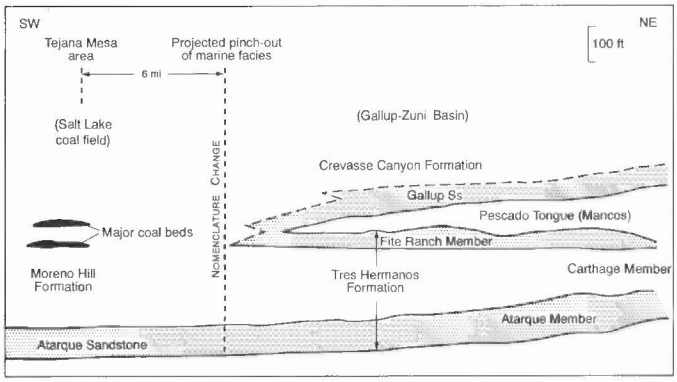

FIGURE 2.30. Stratigraphic diagram of Upper Cretaceous strata in the Salt Lake coal field.

Thus, the lithostratigraphy, timing and extent of the Moreno Hill-Atarque progradation is relatively well understood, even as to first cause. It is, however the subsequent transgression that complicates the stratigraphy and nomenclature of Turonian rocks at Tejana Mesa and areas to the immediate northeast. This transgression brought the strandline back into west-central New Mexico, into the southernmost part of the Gallup-Zuni basin to the Fence Lake area. Projection of the high-stand shoreline along depositional strike (southeast) brings marine water to within 6-8 mi northeast of Tejana Mesa. Thus, Tejana Mesa was within the coastal strip where paralic peat swamps were likely to exist. Coal resource evaluation work by the New Mexico Bureau of Mines and Mineral Resources (Campbell and Roybal, 1984; Anderson, 1987; Campbell, 1989), and the Salt River Project have determined that the thickest coals in this area occur in pods whose axes parallel this paleoshoreline. Stratigraphically these thicker coal beds are correlative with the marine strata to the northeast, which represent high-stand conditions.

The presence of the marine facies to the northeast warranted a separate nomenclature (Fig. 2.30) to properly address the lithostratigraphic expression of a major change in depositional environments (marine encroachment into a coastal plain environment). In areas where the marine influence is present and mappable the name Tres Hermanos Formation is applied to the regressive-transgressive wedge of sediments that is partly equivalent to the Moreno Hill-Atarque sequence (Hook et al., 1983). The Atarque Sandstone is the direct equivalent of the basal sandstone member of the Tres Hermanos Formation, which is called the Atarque Member. The overlying coastal-plain unit (Carthage Member) is equivalent to the lower part of the Moreno Hill Formation. The uppermost Tres Hermanos unit is a fossiliferous, littoral sand of highly variable thickness called the Fite Ranch Member. The exact point of the landward pinchout of the Fite Ranch is not known because the area where this feature would crop out has been truncated by Tertiary erosion; subsurface information has been of little help in defining the pinchout. Based on rate of thinning of the overlying Pescado Tongue of the Mancos Shale, Anderson (1987) projected a landward pinchout of the offshore mudstone facies near the Atarque area (9 mi north of Fence Lake). Depending on width of the littoral zone and shoreline trend the seaway could have been within 6 mi of Tejana Mesa during latest middle to early late Turonian time. An additional significant aspect of this landward pinchout is that it represents the point at which the Gallup regression began. The Gallup Sandstone, a more widespread regressive littoral sand, is a well-known, cliff-forming unit in the southern San Juan basin. The Gallup and its associated, overlying coastal plain depositional sequence, the Crevasse Canyon Formation, represent a response to a eustatic fall of sea level and/or renewed tectonism in the Sevier Orogenic belt in Utah.

The arbitrary line between the two sets of nomenclature, Atarque-Moreno Hill in the Tejana Mesa area and the Salt Lake coal field, versus Tres Hermanos Formation-Pescado Tongue-Gallup-Crevasse Canyon Formations to the northeast, is best drawn at the prominent northwest-trending dike system that runs from just west of Pie Town to the abandoned community of Techado. From there northwestward to the Atarque area the presence of the Pleistocene North Plains basalt flow separates the areas in which the contrasting nomenclature is used. Arbitrary lines between contrasting sets of nomenclature for correlative rocks is a necessity in areas with significant lateral facies change. These areas commonly include intertongued marine-nonmarine rocks such as we find in the Upper Cretaceous in west-central New Mexico and adjacent areas.

57.8 Junction with US-60. **Turn right (west) on US-60. 0.1**

57.9 Low-relief upper Quaternary alluvium in valley bottom is inset against older alluvium (Plio-Pleistocene Quemado Formation) along valley margin ahead. **0.2**

58.1 Road ascends older valley-fill deposits (Quemado Formation), which are exposed in roadcuts next 1.1 mi. **1.2**

59.3 Roadcut exposes Baca Formation on left. Quemado Formation is erosionally inset against the Baca Formation here. **0.1**

59.4 Quemado Formation in right roadcut. **0.4**

59.8 Baca Formation in roadcuts. **0.3**

60.1 Light-colored sandstone of lower Spears Group (upper Eocene) overlain by conglomerate of the Fence Lake Formation (middle to upper Miocene) at 1:00. Highway curves to left and enters Armstrong Canyon. **0.3**

60.4 Exposures of Spears Group at 9:00. **0.1**

60.5 Exposures of Spears Group in roadcuts next 1.5 mi. **1.7**

62.2 Highway crosses covered contact between Spears Group and Fence Lake Formation. **0.1**

62.3 Picnic area on right. **0.4**

62.7 Gravels of Fence Lake Formation capped by prominent calcareous paleosol in roadcuts (Fig. 2.31). **0.1**

62.8 Microwave tower on right. Highway traverses remnant of Fence Lake constructional surface next 0.4 mi. This surface is part of a drainage divide between two Quemado-age paleovalleys (Largo Creek Basin to east; Red Hill Basin to west; see Cather and McIntosh, this volume). **0.7**

63.5 Enter closed basin floored with Quaternary alluvium. Fox Mountain on skyline at 10:00 consists of volcaniclastic deposits of Spears Group overlain by andesite of Dry Leggett Canyon. **0.3**

63.8 Quaternary alluvium in roadcuts. **0.7**

64.5 Road ascends western margin of closed basin. **0.5**

65.0 Roadcuts expose calcareous paleosol developed on Fence Lake Formation. **0.2**

65.2 Highway traverses poorly exposed Fence Lake Formation. **0.5**

65.7 Fence Lake Formation in roadcuts. **0.1**

65.8 Approximate location of contact between Fence Lake Formation and underlying Spears Group. **0.3**

66.1 Roadcuts in Spears Group. Fence Lake Formation caps hill to right. **0.3**

66.4 Highway descends into broad, broken lowland ahead. This is a good vantage point to view part of a large, heretofore unrecognized, erosional basin (or broad paleovalley) of Plio-Pleistocene age in which large volumes of sedimentary and volcanic rocks have accumulated (Cather and McIntosh, this volume). The basin (Red Hill Basin) is geographically quite large. The highlands along the southern boundary occupies much of the skyline to the south and southwest, including the Gallo Mountains (9:00), Fox Mountain (9:30) and Black Peak (10:00). Part of the northern boundary of the basin is visible along the northwestern skyline between about 1:00 and 2:00. The basin (paleovalley) exited to the northwest near Red Hill and Cimarron Mesa. The sedimentary rocks in the basin are partially equivalent to the upper Bidahochi Formation and have been termed the Quemado Formation (Cather and McIntosh, this volume). **0.4**

66.8 Roadcut on left exposes Quemado Formation. **0.3**

67.1 Quemado Formation sandstone and siltstone in roadcuts. **0.5**

67.6 Quemado Formation sandstone in roadcuts, next mile. **1.0**

68.6 Quemado Formation containing minor basaltic gravels exposed in roadcuts. **0.4**

69.0 Most hills in the middle distance 9:00 to 11:00 consist of Plio-Pleistocene basaltic volcanic rocks that overlie or interfinger with the Quemado Formation. **0.2**

69.2 Sands and gravels of Quemado Formation in roadcuts contain weakly developed calcareous paleosoil (Fig. 2.32). These roadcuts have been designated a reference area for the Quemado Formation by Cather and McIntosh (this volume). **0.9**

70.1 Ridge 12:30 to 2:00 consists of Baca Formation overlain by Fence Lake Formation and capped by upper Miocene(?) basalt. This ridge was eroded approximately

FIGURE 2.31. Roadcut exposure of caliche-coated pebbles of Fence Lake Formation.

FIGURE 2.32. Calcareous paleosol in sandstone and siltstone of Quemado Formation in north roadcut of US-60.

to its present morphology before deposition of the Quemado Formation, which laps around the hill on three sides. The low-relief area in the foreground 12:00 to 3:00 is underlain by Quemado Formation and intercalated basalts. **0.1**

70.2 Quemado Formation in left roadcut. **0.2**

70.4 Quemado Formation and intercalated basalt in roadcuts. This basalt has yielded an $^{40}Ar/^{39}Ar$ age of 1.51 ± 0.01 Ma (McIntosh and Cather, this volume). **0.3**

70.7 Milepost 20. **0.1**

70.8 Quemado Formation in roadcuts contains abundant well-rounded quartzite, chert, and other pebbles recycled from the Eocene Baca Formation. Such pebbles are widespread in the Quemado Formation near the northern margin of the basin. **0.4**

71.2 Red beds exposed beneath basalt at 2:00 are Baca Formation. **0.1**

71.3 Quemado Formation in roadcuts. **0.4**

71.7 Quemado Formation in roadcuts overlain by thin mantle of Quaternary cinders. **0.4**

72.1 Upper Miocene(?) (pre-Quemado Formation) basalt overlies lower Spears Group on ridge and in slumped blocks 9:30 to 11:30. **0.9**

73.0 Quemado Formation sandstone and mudstone in roadcuts. **0.3**

73.3 Weakly dissected Quaternary alluvium forms floor of valley. Low hills 8:00 to 11:00 are poorly exposed Quemado Formation. **0.2**

73.5 Exposures of Baca Formation red beds 1:00 to 2:00. **0.4**

73.9 Quemado Formation sandstone and conglomerate in roadcuts. **0.5**

74.4 Cimarron Mesa (12:30-2:00) consists of upper Cretaceous Moreno Hill Formation and Baca/Eagar Formations overlain by Fence Lake gravels and capped by upper Miocene basalt. Preliminary petrographic study of volcanic cobbles, which compose ~ 15% of clasts in the Baca/Eagar Formations here, suggests that many are derived from the Proterozoic metavolcanic terrane of central Arizona (Fig. 2.33). The basal basalt flow along the southwest margin of Cimarron Mesa yielded a $^{40}Ar/^{39}Ar$ age of 6.05 ± 0.02 Ma (McIntosh and Cather, this volume). The area around Cimarron Mesa contains the poorly understood interfingering (?) of volcanic-bearing sandstone and conglomerate of the Eagar Formation and the laterally equivalent, volcanic-free Baca Formation (Cather et al., this volume). Cimarron Mesa (Fig. 2.34) forms an "island" within the Quemado Formation, which surrounds and laps against it on all sides. Road traverses low-relief surface developed on Quemado Formation next 2.0 mi. **0.3**

74.7 Milepost 16. **1.1**

75.8 Roadcuts in Quemado Formation capped by Quaternary cinders. **0.4**

76.2 Quarry for volcanic cinders at 9:00 (Fig. 2.35). Cinders were erupted from a Quaternary cinder cone with a maar about 0.6 mi southwest of here (Quemado crater of Hoffer and Corbitt, 1989). **0.2**

76.4 **Turn left** on road to Luna. **0.1**

76.5 Cinder quarry at 9:00. **0.4**

76.9 Fox Mountain (11:00) is a horst of andesite of Dry

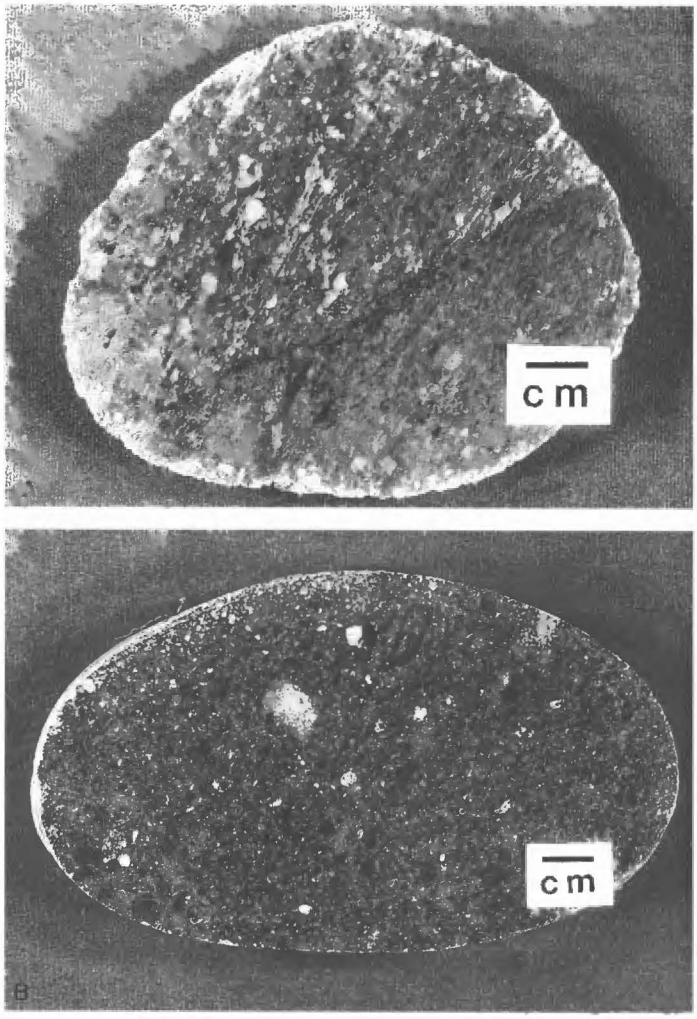

FIGURE 2.33. Slab of siliceous metavolcanic cobbles collected from the Eagar Formation on the east flank of Cimarron Mesa, (SE¼ sec 33, T1N, R19W) A, foliated and sheared metarhyolite lava that contains phenocrystic quartz and recrystallized potassium feldspar. B, rhyolitic metaignimbrite containing dark pumice fiamme (top, right of center), small quartz eyes and angular rock fragments. The Proterozoic metavolcanic terrane in central Arizona is the most likely source.

FIGURE 2.34. View north of Cimarron Mesa from north rim of Quemado crater. Cimarron Mesa is capped with late Miocene (6.05 ± 0.02 Ma) vents and basalts, which overlie Cretaceous and Eocene strata. Note cinder cone within unnamed maar in foreground.

FIGURE 2.35. Quarry developed in Quaternary cinder deposit. Cinders were derived from cone about 0.6 mi to southwest (Quemado crater).

Leggett Canyon overlying volcaniclastic strata (gray cliffs) of the Spears Group. Isolated exposures of Baca Formation occur northeast of Fox Mountain along Demetrio Creek. Cerro la Mula (Fig. 2.36) at 11:45 is a late Pliocene eruptive center that appears to lie along the same fracture system as the vent at El Porticito (Stop 2). A flow on the south flank of Cerro la Mula has been dated 1.947 ± 0.052 Ma (McIntosh and Cather, this volume). **0.4**

77.3 Turn right on two-track road. **0.4**

77.7 Cinder cones at 1:00 and 2:30. **0.2**

77.9 Quemado crater, a Quaternary maar/cinder cone complex, on left. A basalt flow exposed in the southwest wall of the crater predates the maar and has been dated 1.55 ± 0.01 Ma (McIntosh and Cather, this volume). **0.1**

78.0 **STOP 3.** Park on left to discuss Quemado crater (Fig. 2.37) and fracture controls on late Cenozoic eruptive centers. **Retrace route to US-60. 1.6**

79.6 Stop sign. **Turn left (west) on US-60. 0.5**

80.1 Quaternary cinder cones at 9:00 (see Hoffer and Corbitt, 1989). **0.2**

FIGURE 2.36. View south of Cerro la Mula, a late Pliocene eruptive center.

80.3 Quemado Formation and Quaternary cinders in roadcuts. **0.3**

80.6 Slight westerly tilts on Plio-Pleistocene(?) basalt flows 9:30 to 11:00 are related to nearby north-northeast-trending normal faults, which are part of a major fault zone of regional extent. These faults commonly control the location of late Tertiary-Quaternary vents throughout this area. **0.9**

81.5 Sandstone and pebbly sandstone of Quemado Formation in roadcuts. **0.3**

81.8 Escudilla Mountain near Alpine, Arizona on skyline at 10:30. **0.7**

82.5 Red Hill cinder cone on skyline at 3:00 is possibly the youngest volcanic feature in the Red Hill-Quemado volcanic field (Fig. 2.38). A basalt that flowed westward from the base of the cone has been dated by $^{40}Ar/^{39}Ar$ geochronometry at 0.071 ± 0.012 Ma (McIntosh and Cather, this volume). **0.1**

82.6 Sandstone and conglomerate of Quemado Formation in roadcuts. Much of the gravel in the Quemado has been reworked from the Fence Lake and Eagar Formations. **0.3**

82.9 Milepost 11. **0.1**

83.0 Quemado Formation in roadcuts. The coarseness of the Quemado here reflects the proximity of the western basin margin (on skyline ahead). **0.2**

83.2 Red Hill, New Mexico. Much of the low-lying topography south and southeast of Red Hill consists of Quemado Formation, which interfingers with and is overlain by Plio-Pleistocene basalts. **0.6**

83.8 Gravel pits at 2:00 to 3:00 expose Eagar Formation and a thick calcrete (Fig. 2.39). Low, rolling topography in foreground is Quemado Formation. **0.8**

84.6 Basalt interbedded with Fence Lake Formation in roadcuts. A sample from this roadcut yielded a $^{40}Ar/^{39}Ar$ age of 5.20 ± 0.03 Ma (McIntosh and Cather, this volume). About 6 mi to the southeast, apparently correlative basalts have been dated at 6.4 ± 0.3 Ma (Baldridge et al., 1989). These upper Miocene basalts and intercalated gravels of the Fence Lake Formation form a paleodivide between the Quemado-age Red Hill Basin to the east and the Cow Springs Basin to the west. **0.5**

85.1 Rolling topography from 8:00 to 4:00 is underlain by upper Miocene basalts and intercalated Fence Lake Formation. Exposures of the Fence Lake Formation extend nearly 12 mi to the north-northwest where they overlie Upper Cretaceous strata. These Fence Lake exposures have been incorrectly mapped as Baca Formation by some previous workers. **0.9**

86.0 Rest area on left. Roadcuts expose gravels of Fence Lake Formation. Upper Miocene (?) basalts cap ridges 1:00 to 3:00. **0.3**

86.3 Entering Cow Springs Basin. Low-lying area at 9:00 to 12:00 is Quemado Formation and interbedded Pliocene basalts. US-60 traverses northeast margin of the Cow Springs Basin next 4 mi. **1.6**

87.9 Milepost 6. Volcaniclastic sandstones in roadcuts. Correlation of these sandstones is ambiguous; they may represent either a fine-grained facies of the Fence Lake Formation or part of the lower Spears Group. **1.1**

89.0 Escudilla Mountain at 10:00. White Mountains at 11:00. Microwave tower on left. **0.7**

FIGURE 2.37. Aerial view of the Quemado crater, looking south. County road to Luna passes left (east) of the crater rim and US-60 passes from lower left to center right. A narrow graben trends south-southwest from the west rim of the crater. An early Pliestocene basalt flow is offset by the graben. A second, unnamed crater is next to US-60 in foreground. Fox Mountain, on the middle skyline, is capped by the andesite of Dry Leggett Canyon (upper Eocene; ~ 34 Ma).

89.7 Basalt-capped peak at 1:30 exposes 30 ft of volcaniclastic conglomerate of the Fence Lake Formation on south slope (Fig. 2.40). Correlation of the buff volcaniclastic sandstones beneath the Fence Lake is ambiguous; these sediments may pertain to the lower Spears Group or to an anomalously fine-grained facies within the Fence Lake Formation. The basalt that caps the Fence Lake conglomerate here was dated 6.03 ± 0.02 Ma using $^{40}Ar/^{39}Ar$ geochronometry (McIntosh and Cather, this volume). **0.3**

90.0 Quemado Formation overlain by Pliocene(?) basalt in left roadcut. **0.6**

90.6 Mesa Redonda on skyline at 11:00 to 1:00 formed a "paleoisland" within the Cow Springs Basin, which exited around both sides of the mesa to the northwest. **0.5**

91.1 Road traverses low-relief landscape underlain by Pliocene basalts and Quemado Formation. **1.5**

92.6 Roadcuts in basalt overlying variegated Quemado Formation beds (Fig. 2.41). The uppermost basalt in the south roadcut yielded a $^{40}Ar/^{39}Ar$ age of 2.46 ± 0.04 Ma (McIntosh and Cather, this volume). This is one of a series of related flows that cap the Quemado Formation type section 6 mi to the north as well as the Bidahochi Formation near Mesa Parada in Arizona about 22 mi to the north-northwest. A basalt that caps a prominent calcareous paleosol developed on the top of the Bidahochi 1.85 mi north-northwest of Mesa Parada has been dated at 2.37 ± 0.03 Ma by the $^{40}Ar/^{39}Ar$ method (McIntosh and Cather, this volume). These relations indicate that the Quemado Formation is at least in part equivalent to the Bidahochi Formation, although the lower Bidahochi is older (late Miocene) and some of the Quemado beds to the east are Pleistocene and appear to post-date the end of Bidahochi deposition. **0.3**

92.9 Roadcut on right in Eagar Formation, which comprises lower part of Mesa Redonda to north. Mesa is capped by Fence Lake Formation and upper Miocene(?) basalt. **0.3**

93.2 Thin sequence of Quemado Formation overlies Eagar Formation in right roadcuts. Quemado is, in turn, overlain by Pliocene basalt, both of which are inset against "paleoisland" mesa on skyline to north (2:00 to 4:00). Mesa-capping Pliocene basalts to west and south are locally underlain by Quemado Formation. **0.4**

93.6 Eagar Formation in right roadcuts. **0.3**

93.9 Rest area on left. Mesa Redonda on skyline at 3:00 is capped by upper Miocene(?) basalt that overlies volcaniclastic conglomerate of Fence Lake Formation

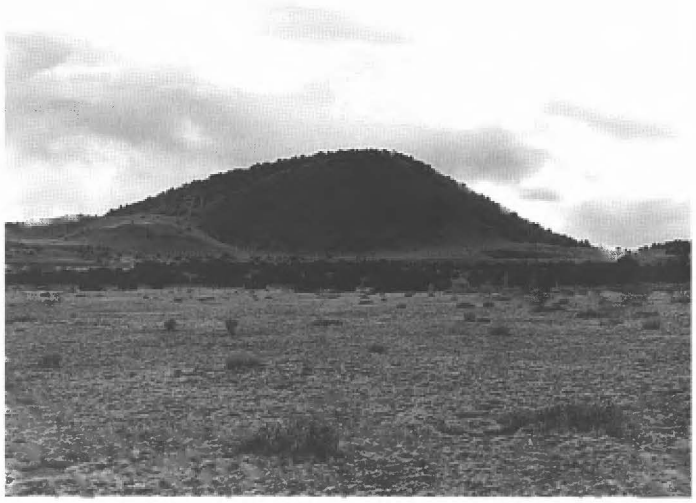

FIGURE 2.38. Northward view of Red Hill cinder cone.

which, in turn, disconformably overlies pebbly volcaniclastic sandstone of the lower Spears Group. **0.1**

94.0 Entering Arizona. With the exception of the upper Cenozoic volcanic rocks of the White Mountains and Springerville volcanic fields, the geology of the remainder of today's field trip has been little studied. As such, the geologic interpretations presented in the remainder of this road log should be regarded as preliminary. **0.7**

94.7 Roadcuts expose variegated Upper Cretaceous mudstone disconformably overlain by conglomerate and sandstone of Eagar Formation (Eocene) and Pliocene basalt. The base of the Eagar here is very coarse; slabs of Cretaceous sandstone about 3 ft long are present in the right roadcut (Fig. 2.42). The top of the Cretaceous section along US-60 in eastern Arizona is highly oxidized and commonly displays reddish hues, particularly in the sandstones. Because of this anomalous coloration, the upper part of the Cretaceous section in this area has been confused with Eocene strata by some workers (see following minipaper). Chamberlin (1981b, 1989) described similar reddened Cretaceous rocks beneath the Baca Formation in west-central New Mexico and ascribed their coloration to the effects of early Tertiary oxidation in a deeply weathered zone prior to the onset of late Laramide sedimentation. Sparse pebbles of Laramide (?) andesite porphyry are present in the basal Eagar beds here. **0.5**

FIGURE 2.39. Stage VI calcrete developed on siliceous cobble conglomerates of the Eagar Formation that are exposed in the north rim of a borrow pit approximately 1.0 mi northwest of Red Hill. This thick calcrete is probably correlative with a late Miocene calcrete commonly found at the top of the Fence Lake Formation.

LOCAL MISAPPLICATION OF THE TERM EAGAR TO UPPER CRETACEOUS STRATA IN EASTERN ARIZONA

Steven M. Cather

New Mexico Bureau of Mines and Mineral Resources, Socorro, NM 87801

Sirrine (1956) named the Eagar Formation and designated the type section in Antelope Valley about 16 km northeast of Springerville, Arizona (N½ sec. 28, T10N, R30E). The type section consists of 473 ft (144 m) of mostly red sandstone and conglomerate. At the type section, the basal part of the Eagar section consists of conglomerate and pebbly sandstone that overlies the Upper Cretaceous Mancos Shale. The top of the Eagar is not exposed at the type section, but elsewhere grades transitionally up-section into mid-Tertiary volcaniclastic sedimentary rocks (termed Spears Group by Cather et al., this volume).

During the course of his dissertation mapping, Sirrine (1956) extended the Eagar Formation east and south of the type locality. In the type area and in other parts of his study area where Upper Cretaceous rocks were not anomalously reddened, Sirrine placed the base of Eagar at the Cretaceous-Tertiary unconformity. In his geologic mapping near the Arizona-New Mexico line in the vicinity of US-60, however, Sirrine (1956) erroneously included a non-conglomeratic sequence of Upper Cretaceous red sandstones and variegated, locally lignitic, mudstones in the basal part of the Eagar Formation. Samples collected from a lignitic coal and overlying shale within this sequence yielded spores and pollen of Late Cretaceous age (R. Y. Anderson, written commun. in Sirrine, 1956). The age implications for these pollen and spores, together with the transitional contact relations with the overlying volcaniclastics, led Sirrine to assign a Late Cretaceous-Paleocene age to the Eagar Formation. Subsequent to the work of Sirrine (1956), paleontological and radiometric studies have indicated an Eocene age for Eagar-equivalent units (Baca and Mogollon Rim Formations) in eastern Arizona and west-central New Mexico (see summaries in Lucas, 1983; Cather and Johnson, 1984; Potochnik, 1989). No further age data have been obtained for the Eagar Formation.

The mapping error near the Arizona-New Mexico line and resultant incorrect age assignment for the lower Eagar by Sirrine has been

FIGURE 2.40. Basalt capping this butte overlies Fence Lake conglomeratic sandstone in exposure on left. Other sandstones below the conglomerates may represent the Fence Lake Formation or Spears Group.

FIGURE 2.41. Late Pliocene basalt flow overlies Quemado Formation at Mile 92.6.

promulgated for many years in the regional literature. As recently as 1971, Snyder attributed a possible Late Cretaceous age to basal Baca-Eagar beds in western New Mexico and eastern Arizona based on Sirrine's work. B. D. Johnson (1978, p. 5) was the first to note the erroneous inclusion of Upper Cretaceous strata in the Eagar Formation. A road log along US-60 just west of the Arizona-New Mexico state line (Anderson et al., 1987) noted the presence of unusually colored Upper Cretaceous strata in the roadcuts; these rocks were mapped as Eagar by Sirrine (1956). Anomalously red Upper Cretaceous rocks have been noted in other localities in western New Mexico beneath the basal Tertiary unconformity (Chamberlin, 1981b; Guilinger, 1982). The red coloration was interpreted by Chamberlin (1981b) to have formed in an oxidized, lateritic weathering zone prior to the onset of Baca-Eagar sedimentation in the Eocene.

In April, 1994, I visited the type section of the Eagar Formation and remapped a small part of Sirrine's study area (Fig. 2.43), being careful not to be misled by anomalous coloration. The Upper Cretaceous Moreno Hill Formation crops out in the lower elevations along Coyote Creek, and is disconformably overlain by the basal conglomerate or conglomeratic sandstone of the Eagar Formation. The unconformity beneath the Eagar shows as much as 100 m of relief within the map area, and is locally angular. Elevation differences between Upper Cretaceous strata along Coyote Creek (all of which was mapped as Eagar by Sirrine, 1956) and volcaniclastics of the Spears Group near the state line indicate an approximate maximum thickness for the Eagar of only 120 m. I also revisited Sirrine's (1956) pollen locality; it is clearly within what I regard as the Upper Cretaceous Moreno Hill Formation (Fig. 2.43). Chamberlin (1981b) and Guilinger (1982) described other Late Cretaceous pollen assemblages from within anomalously reddened Mesaverde Group outcrops beneath the basal Tertiary unconformity in areas nearby to the east.

FIGURE 2.42. Boulder of Upper Cretaceous sandstone marks conglomeratic base of Eagar Formation at Mile 94.7.

I have found the following lithologic criteria are useful in distinguishing red Upper Cretaceous strata from the overlying Eocene rocks in west-central New Mexico and eastern Arizona. *Presence of conglomerate:* Conglomerate is common in the Eocene strata, whereas Cretaceous rocks, with the exception of intraformational mudclasts, are not coarser than very coarse sandstone. *Coloration of mudstones:* Cretaceous mudstone units are commonly variegated and preserve remnants of "typical" Cretaceous gray to maroon coloration (Chamberlin, 1981b) and lignite. The great majority of Eocene mudstones are uniformly red. *Sandstone characteristics:* Cretaceous sandstones are typically more thickly bedded and more texturally uniform than Eocene sandstones. Cretaceous sandstone beds typically contain large-scale trough cross-stratification, whereas small- to medium-scale trough and tabular cross-stratification and horizontal stratification is more common in Eocene sandstones.

95.2 Anomalously red Upper Cretaceous sandstone of Moreno Hill Formation in quarry at 9:00. **0.3**

95.5 Variegated mudstone and red sandstone of Moreno Hill Formation in roadcuts (Fig. 2.44). **0.1**

95.6 Crossing Coyote Creek. Many of the red rocks in the lower elevations along Coyote Creek 1:00 to 4:00 are Upper Cretaceous. **0.3**

95.9 Milepost 400. **0.1**

96.0 Roadcuts expose red conglomerate, sandstone and mudstone of Eagar Formation. **0.3**

96.3 Conglomerate, sandstone, and mudstone of Eagar Formation in roadcuts (Fig. 2.45). **0.6**

96.9 Milepost 399. Escudilla Mountain at 9:00. White Mountains 10:00 to 1:00. **0.6**

97.5 Roadcuts expose red mudstone and grayish pink conglomerate and conglomeratic sandstone of Eagar Formation, next 1.5 mi. **2.1**

99.6 Quaternary alluvium exposed in roadcuts. **1.2**

100.8 Red sandstone and mudstone of Eagar Formation exposed in roadcuts. **0.7**

101.5 Roadcuts expose red mudstone of Eagar Formation overlain by buff sandstone and conglomerate of the Quemado(?) Formation. These are, in turn, overlain by a basalt flow dated 3.67 ± 0.12 (whole-rock K/Ar age, Laughlin et al., 1980). A prominent calcareous paleosol intervenes between the Quemado(?) and the basalt (Fig. 2.46). The buff-colored strata beneath the basalt are tentatively correlated with the upper Bidahochi Formation on the basis of their position in the landscape, lithology, and the presence of a capping Pliocene basalt. **0.5**

102.0 Milepost 394. Coyote Hills (Fig. 2.47), a Pleistocene shield volcano (0.82 ± 0.04 Ma; Crumpler et al., this volume), is at 1:00. **0.6**

102.6 Pliocene(?) basalt in roadcuts. **0.7**

103.3 Quemado(?) Formation in right roadcut. Gravel and cinder quarry on right. View to southwest (10:00) shows progressively older basalts occupying higher positions in the landscape (Fig. 2.48). Mesa slightly below road level at 9:00 (elevation 7285 ft; middle distance on right of photo) is capped by two flows dated 2.94 ± 0.14 Ma and 0.824 ± 0.040 Ma (Laughlin et al.,

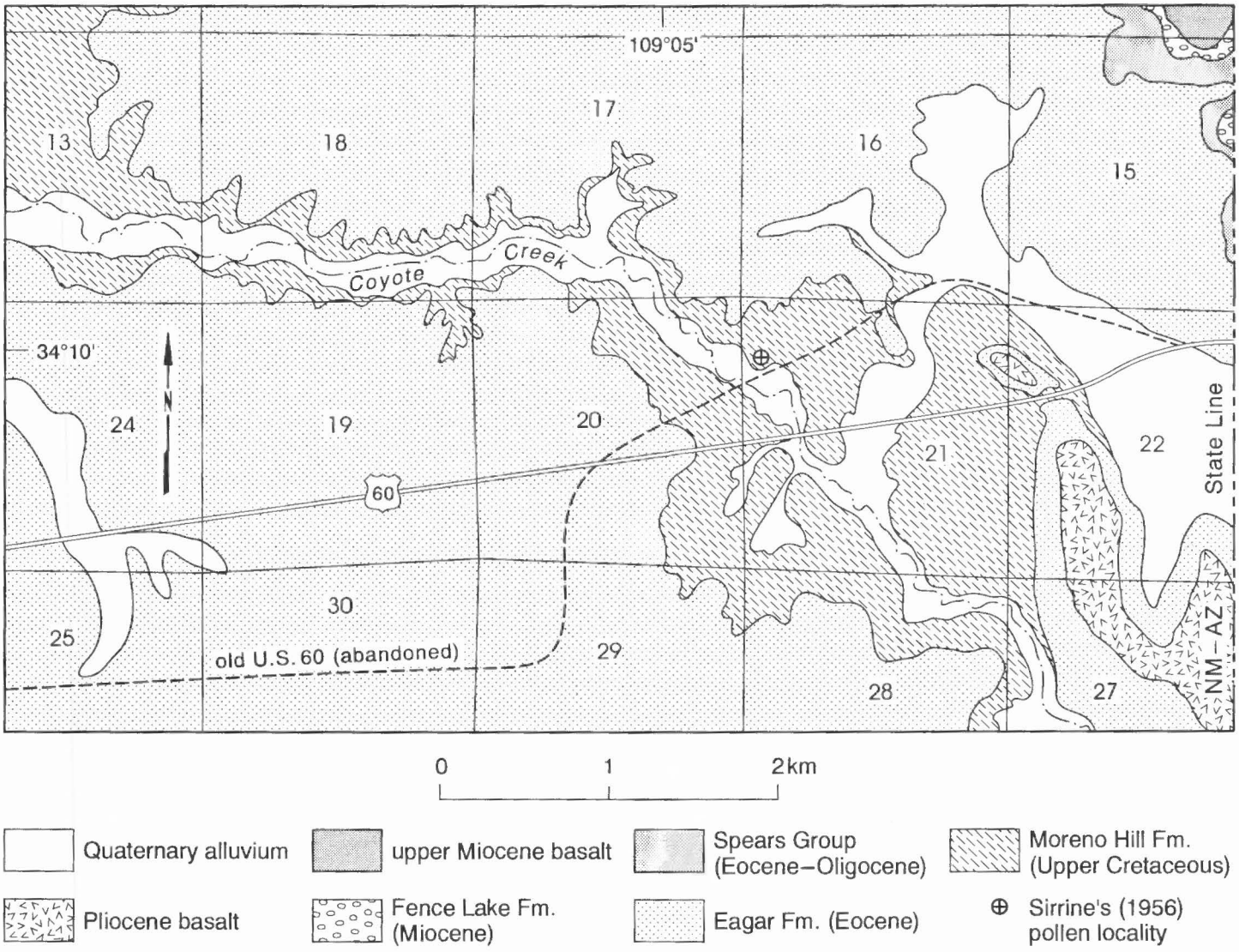

FIGURE 2.43. Reconnaissance geological map of the Coyote Creek area, east-central Arizona. Mapped by S. M. Cather during March 1994.

1979). The unnamed mesa in middle ground to left at 9:00 to 10:30 (elevation 7580 ft) is capped by 3.87 ± 0.10 Ma basalt where it is surmounted by US-180 about 3.7 mi south-southwest of here (Laughlin et al., 1980). The mesa at 10:30 (Flat Top, in center of photo, elevation 8070 ft) is capped by 6.80 ± 0.02 Ma basalt (McIntosh and Cather, this volume). The White Mountains (elevation 11,150 ft) on the distant skyline at 11:00 are composed of volcanic rocks of mostly late Miocene age. The inset nature of the progressively younger basalts visible from here illustrate the net degradation which has occurred in this area at least since the late Miocene. **0.2**

103.5 Springerville, Arizona visible through canyon at 11:00. **0.4**

103.9 Basalt in roadcuts. **0.2**

104.1 Rest area on left. Mesa on skyline at 9:30 exposes Eagar Formation red beds and thin Quemado(?) Formation overlain by Pliocene basalts. Begin downgrade into Round Valley. **0.4**

104.5 Roadcuts expose two basalt flows separated by a thin sandstone and conglomerate unit (Quemado Formation?). The lower basalt here was dated at 2.94 ± 0.14 Ma; the upper flow is 0.824 ± 0.040 Ma (Laughlin et al., 1979). **0.4**

104.9 Red beds of Eagar Formation in roadcuts. **0.3**

105.2 Eagar Formation in roadcuts. **0.3**

105.5 Quaternary alluvium, deposited along the upper reaches of the Little Colorado River and its tributaries, comprises the low-relief floor of Round Valley. **0.5**

106.0 Quaternary alluvium in roadcuts. **0.3**

106.3 Entering Springerville. Western part of Springerville volcanic field (11:00 to 1:00) consists dominantly of alkali olivine basalt erupted mainly from monogenetic cinder cones during latest Pliocene to Pleistocene time (Condit et al., 1989; Crumpler et al., this volume). The White Mountains volcanic field occupies the high ground at 10:00 to 11:00 and is distinctly older (late Miocene) than the Springerville field. **0.9**

107.2 **Turn left** on US-180/US-191. **0.8**

108.0 Flat Top Mesa (Fig. 2.49) at 1:00 consists of a thick sequence of Eagar Formation overlain by late Miocene

FIGURE 2.44. Variegated mudstone and red sandstone of Upper Cretaceous Moreno Hill Formation in north roadcut of US-60. Reddening of permeable sandstones occurred within deeply weathered zone prior to onset of Eocene deposition (Chamberlin, 1981).

FIGURE 2.46. Calcareous paleosol developed at top of Quemado(?) Formation in north roadcut of US-60, overlain by Pliocene basalt.

FIGURE 2.45. Eagar Formation conglomerate and conglomeratic sandstone fills paleochannel incised into red Eagar mudstone in roadcut at Mile 96.3.

FIGURE 2.47. View northwest of Coyote Hills, a Pleistocene shield volcano.

6.80 ± 0.02 Ma basalt (McIntosh and Cather, this guidebook). On the basis of float found along the northeast side of the mesa, it appears that a thin (<30 ft), gravelly, upper Tertiary unit intervenes between the basalt and the Eagar Formation. This gravel may correlate with the Fence Lake Formation of west-central New Mexico, based on its lithology, position in the landscape, and the age of the capping basalt. **1.3**

109.3 Stop sign at intersection. **Turn left on US-180/US-191. 1.0**

110.3 Entering Apache National Forest. **0.7**

111.0 Roadcuts expose red beds of Eagar Formation disconformably overlain by upper Tertiary volcaniclastic gravels (Quemado Formation?). Conglomerate in the Eagar Formation here contains subequal volcanic and non-volcanic clasts. A significant but unknown part of the volcaniclastic detritus in the Eagar may be derived from older volcanics (Laramide, Jurassic, or Proterozoic) to the south, as opposed to being the record of incipient mid-Tertiary volcanism. In the eastern Baca basin, the transition between the largely non-volcanic, orogenic deposits of the middle to upper Eocene Baca Formation and the overlying andesitic volcaniclastics of the upper Eocene Spears Group is commonly defined by the first up-section occurrence of megascopically visible volcanic detritus (Cather, 1980; Cather and Johnson, 1984). Such a demarcation is not feasible, however, in the western part of the Baca basin, where the synorogenic Eagar and Mogollon Rim Formations contain significant amounts of volcanic detritus throughout. This situation led Potochnik (1989) in areas to the west to draw the upper contact of the Mogollon Rim Formation where volcanic detritus becomes volumetrically dominant (>50%). A similar approach probably would be best in the Springerville area. Because the lithologic transition between the Eagar Formation and the overlying Spears Group Formation is stratigraphically quite broad and relatively fine-grained, definitive placement of the contact between these units must await detailed mapping. The placement of the contact in this road log is quite approximate and is based solely on cursory hand-lens estimation of the detrital composition of Eagar-Spears sandstones. **0.6**

FIGURE 2.48. View to southwest showing progressively older basalts occupying increasingly high positions in the landscape. See text for age of basalt flows.

FIGURE 2.50. Two basalt flows exposed in canyon of Nutrioso Creek. Upper basalt is early Pliocene in age, as it appears to correlate with dated basalt nearby to west (3.87 ± 0.10 Ma; Laughlin et al., 1980). Lower basalt is undated and appears to have flowed down paleocanyon of ancestral Nutrioso Creek.

111.6 A thin sequence of Quemado(?) gravels intervenes between the red beds of the Eagar Formation and the capping basalt of Pliocene age (3.87 ± 0.10 Ma; Laughlin et al., 1980). **0.6**

112.2 Eagar Formation and Pliocene basalt in left roadcut. **0.6**

112.8 Milepost 406. Left roadcuts expose Eagar Formation. **0.5**

113.3 Two basalt flows are visible across canyon at 11:00 to 12:00 (Fig. 2.50). The upper, mesa-capping flow is of Pliocene age. The lower (younger) flow appears to be inset along a paleocanyon of ancestral Nutrioso Creek, but has not been dated. **0.5**

113.8 Highway follows Nutrioso Creek. Roadcuts on right in Eagar Formation (Fig. 2.51) next 1.0 mi. **1.2**

115.0 Roadcut ahead on right is Eagar Formation. Young basalts near road are inset against older basalt, which caps mesa at 11:00. **0.7**

115.7 Approximate contact between Eagar Formation and overlying, dominantly volcaniclastic Spears Group in left roadcut. **0.3**

116.0 Roadcuts on left in Spears Group next 1.4 mi. Nelson Reservoir Recreation Site on right. **1.8**

117.8 Basalt-capped mesas on left and right. **0.2**

118.0 Spears Group in left roadcut. **0.2**

118.2 Escudilla Mountain at 11:00 is capped by Bearwallow Mountain Andesite (24–26 Ma). Prominent pine-covered bench about half way up the mountain consists of andesite of Dry Leggett Canyon (~34 Ma). Mesa in foreground is capped by Pliocene(?) basalt. Light-colored cliffs at 12:30 are Spears Group; this unit forms the gentle slopes on Escudilla Mountain and is largely eolian in its upper part above the andesite of Dry Leggett Canyon (Wrucke, 1961). Clasts of Precambrian red granite and Paleozoic limestone occur in the Spears Group below the andesite of Dry Leggett

FIGURE 2.49. View of Flat Top Mesa, which consists of a thick sequence of Eagar Formation capped by 6.80 Ma basalt. A thin sequence (<10 m) of gravels underlies the basalt and may correlate with the Fence Lake Formation.

FIGURE 2.51. Sandstone, siltstone and lenticular conglomerate in upper Eagar Formation exposed at Mile 113.8.

Canyon unit and may indicate part of the transition with the underlying Eagar Formation. Road is on Quaternary alluvium in Nutrioso Creek valley. **0.7**

118.9 Milepost 412. Light-gray cliffs at 11:00 and 12:00 are Spears Group. Skyline cliffs at 11:30 are andesite of Dry Leggett Canyon. **1.8**

120.7 Spears Group in left roadcut and in light gray cliffs at 11:00. **1.6**

122.3 Light gray cliffs of Spears Group at 10:00 to 11:00 and 2:00 to 3:00. **1.3**

123.6 Road to Nutrioso on left. Continue straight ahead on US-180/US-191. **0.9**

124.5 Roadcuts contain Spears Group (locally capped by Quaternary gravels) next 0.5 mi. **0.3**

124.8 Sawmill on left. Cliffs beyond sawmill are Spears Group (light gray) capped by andesite of Dry Leggett Canyon. **0.3**

125.1 Milepost 418. **0.3**

125.4 Roadcuts expose Spears Group. **0.4**

125.8 Road to Nutrioso on left. **0.7**

126.5 Roadcuts in Spears Group next 2.7 mi. **2.7**

129.2 Highway surmounts saddle at Alpine Divide (part of Rim Divide of Cather et al., this volume). Drill pad for Alpine 1 Federal corehole on left. **STOP 4. Park on shoulder** to discuss stratigraphy in corehole and regional petroleum and geothermal implications. **Obey flagmen and beware of traffic**.

The Alpine 1 Federal (Fig. 2.52), collar elevation of 8556 feet, was a slim-hole test cored to 4505 feet depth to evaluate the eastern White Mountains region as a site for near-term commercial Hot Dry Rock (HDR) geothermal utilization. Temperature gradients between 60 and 75°C/km characterize the hole in the upper 2500 feet in sediments of relatively low thermal conductivity. Temperature gradients below 2500 feet in relatively high conductivity rocks range from 48 to 32°C/km. A bottom-hole temperature of 173°F (78°C) was recorded. A preliminary heat-flow estimate is between 90 and 100 mWm^{-2} (John Sass, personal commun., 1993). This heat flow is more typical of the Basin and Range rather than the Colorado Plateau. However, the heat flow may be a part of a pattern of local high anomalies, superimposed on a region of intermediate heat flow, similar to the observations of Minier and Reiter (1991) and Minier et al., (1988) on the Mogollon slope in adjacent New Mexico.

A qualitative potential for petroleum in the area is indicated by shows of oil in the core. Carbon-rich Cretaceous sandstones and fetid and petroliferous dolomites and limestones in the Permian San Andres and the Supai/Yeso strata beneath the Glorieta indicate source-rock potential. Important formation breaks (Table 2.1) include the base of the Spears Group at 2052 ft, base of the Eagar Formation at 3139 ft, top of the Cretaceous Dakota (?) at 3246 ft, and the top of the San Andres at 3362 ft. Basalt intrusions obscure formation tops of underlying Permian units. The deepest observed Glorieta Sandstone is at 3639 ft in contact with a basaltic intrusion. The top of the Fort Apache Limestone member (Winters, 1963) is intruded by a basaltic intrusion. The base of the Permian Fort Apache Limestone occurs at 4405 ft. At total depth, the Alpine 1

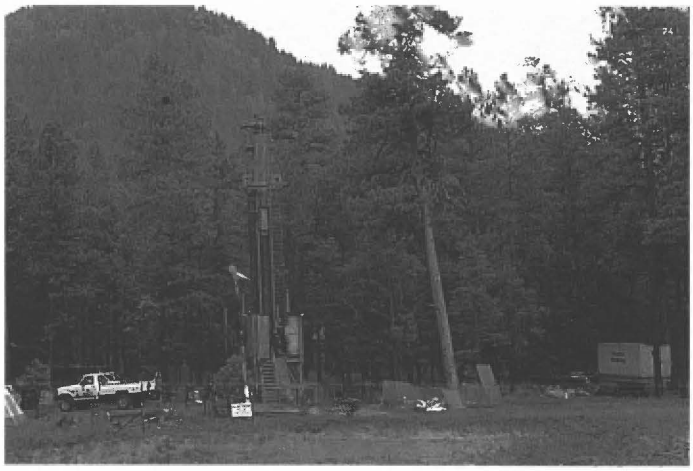

FIGURE 2.52. Drill rig for geothermal test well at the Alpine Divide, east side of US-191 at an elevation of 8556 ft, August, 1993.

TABLE 2.1. Formation summary of the Alpine 1/Federal corehole (see Mile 129.2).

Eocene-Oligocene lower and middle Spears Group
0 to 2052 feet (0-625 m)
thickness 2052 feet (625 m)
Eocene-Eagar Formation
2052 to 3,139 feet (625 to 957 m)
thickness 3,139 feet (957 m)
Unnamed Tertiary (?)/Cretaceous(?) unit
3,139 to 3,226 feet (957 to 989 m)
thickness 107 feet (32 m)
Cretaceous Dakota(?) Sandstone (upper 20 ft [6 m] is reddened)
3,226 to 3,362 feet (989 to 1,025 m)
thickness 116 feet (36 m)
Permian San Andres Formation
3,362 to 3,436 feet (1,025 to 1,047 m)
thickness 74 feet (22 m)
Permian Glorieta Sandstone
3,436 to 3,639 feet (1,047 to 1,109 m)
thickness 203 feet (62 m)
Quaternary(?)/Tertiary(?) basaltic intrusion
3,639 to 3,751 feet (1,109 to 1,143 m)
thickness 112 feet (34 m)
Permian Corduroy member Supai Formation
3,751 to 4,266 feet (1,143 to 1,298 m)
thickness 515 feet (157 m)
Quaternary(?)/Tertiary(?) basaltic intrusion
4,260 to 4,322 feet (1,298 to 1,317 m)
thickness 62 feet (19 m)
Permian Fort Apache Limestone member Supai Formation
4,322 to 4,327 feet (1,317 to 1,319 m)
thickness 5 feet (2 m)
Quaternary(?)/Tertiary(?) basaltic intrusion
4,327 to 4,362 feet (1,319 to 1,330 m)
thickness 35 feet (11 m)
Permian Fort Apache Limestone member Supai Formation
4,362 to 4,405 feet (1,330 to 1,343 m)
thickness 43 feet (13 m)
Permian Big A Butte member Supai Formation
4,405 to 4,454 feet (1,343 to 1,358 m)
thickness 49 feet (15 m)
Quaternary(?)/Tertiary(?) basaltic intrusion
4,454 to 4,505 feet (1,358 to 1,373 m)
thickness 51 feet (15 m)

Federal corehole is in a basaltic intrusion. It is uncertain if the intrusions are the result of late Tertiary magmatic activity, associated with the White Mountains volcanic field centered 20 mi west of the Alpine Divide location, or with older mid-Tertiary activity of the Mogollon-Datil field, or with even younger Plio-Pleistocene activity of the Springerville field. The following minipapers by Witcher et al. describe the geothermal potential of the Alpine area and delineate the constraints on regional maturation of hydrocarbons. **0.2**

THERMAL REGIME OF ALPINE DIVIDE AND PETROLEUM IMPLICATIONS

James C. Witcher[1], Chandler A. Swanberg[2], and W. Richard Hahman[3]

[1]New Mexico State University, Southwest Technology Development Institute, Las Cruces, NM, 88003; [2]Consultant, 5478, E. Cholla St., Scottsdale, AZ 85254; [3]Consultant, 780 Suzanne Ave., Las Cruces, NM 88005

Numerous shallow (<0.5 km) heat-flow measurements have been reported in the region around Alpine Divide (Minier et al., 1988; Minier and Reiter, 1991; Reiter and Shearer, 1979; Sass et al., 1982; and Stone, 1980). Minier and Reiter (1991) described the shallow heat flow in the region as a pattern of local high (>90 mW/m^2) anomalies interspersed over a region of low-to-intermediate (<70 mW/m^2) heat flow. No regional trend in heat flow is apparent. However, high heat-flow measurements tend to be located near local zones or trends of folding and faulting. Minier and Reiter (1989) discussed the thermal regime in terms of fairly uniform coal maturation indices at different locations across the region. A preliminary heat flow for the Alpine 1/Federal corehole at Alpine Divide is 90 mW/m^2 (J. H. Sass, personal commun., 1994)

Heat-flow information for the area allows a provisional assessment of petroleum potential with respect to the results of the Alpine 1/Federal corehole. Oil shows in Permian carbonate rocks may indicate petroleum resource potential in the region (Rauzi, 1994a b; Witcher et al., this volume). To assess the importance of the oil shows, it is necessary to understand the burial and thermal history of potential source rocks. Time and temperature are key factors in oil generation and destruction. For each 10°C increase in temperature, maturation rates roughly double (Waples, 1980). Oil shows may indicate that the Permian source rocks are in the oil-generation window, or that oil has migrated into these rocks from elsewhere in the area or from greater depth. A third possibility is that the oil shows represent limited-volume, local generation from the thermal effects of the basaltic intrusions.

Lopatin's method provides insight into the nature and degree of maturation of potential source rocks (Waples, 1980). Two Lopatin models are presented. Model 1 (Fig. 2.53) investigates the time-temperature index (TTI) of hydrocarbon maturity for the Alpine Divide source rocks. Model 2 (Fig. 2.54) investigates oil generation in a hypothetical late Tertiary extensional basin that is superimposed on the pre-Miocene geology of Alpine Divide. The second model may provide an analog for conditions in grabens to the south and east, provided Permian and Pennsylvanian rocks have not been removed by erosion beneath a Laramide unconformity, and provided heat flow and thermal history are similar to Alpine Divide.

Several assumptions are used in both models. First, heat flow and surface temperature varied with time. The average present Colorado Plateau heat flow is about 68 mW/m^2 (Eggleston and Reiter, 1984; Morgan and Gosnold, 1988; Reiter and Clarkson, 1983). The average worldwide average heat flow is 60 mW/m^2. A 60 mW/m^2 heat flow is used from the Pennsylvanian until the end of the Oligocene in the maturation models. Actual heat flow probably varied between 50 and 70 mW/m^2 during this time frame as a result of uplift, sedimentation, and changes in tectonic setting. Today's heat flow of 90 mW/m^2 is used

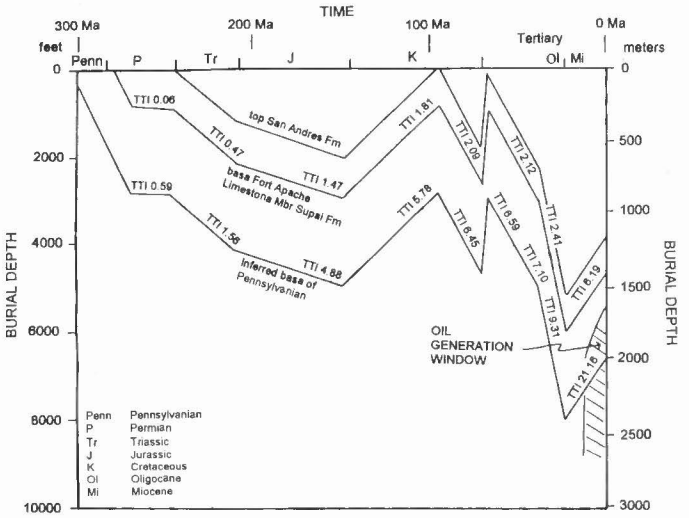

FIGURE 2.53. Lopatin maturation model for Alpine Divide. Lopatin time-temperature index (TTI) of organic matter maturity is shown at various times for the Fort Apache Limestone Member burial curve and the burial curve for the base of inferred Pennsylvanian rocks. Temperatures were calculated from the heat flow, thermal conductivity and surface temperature assumptions. Pennsylvanian to mid-Tertiary heat flow is 60 mW/m^2. Post-Oligocene heat flow is 90 mW/m^2. Thermal conductivity estimates are 2.8 W/mK for Paleozoic and Mesozoic carbonate and quartzose sandstones, 2.2 W/mK for Jurassic rocks, 1.8 W/mK for Eocene clastic rocks, and 1.4 W/mK for the Triassic Chinle and Oligocene volcaniclastic rocks. Surface temperatures are 30°C for the Paleozoic and Triassic, 25°C for the Jurassic and Cretaceous, 15°C for the Eocene and Oligocene, and 10°C for Miocene to present.

from the end of Oligocene until present. This value may be high for the early and mid Miocene, but it provides an upper constraint on late Tertiary maturation history. Surface temperatures are allowed to range from 30°C in the Paleozoic to 10°C in late Tertiary. Sabkha depositional environments during Permian indicate a hot dry climate (Witcher et al., this volume). Present mean annual temperature at Alpine Divide is less than 10 C.

While no Triassic or Jurassic rocks exist in the subsurface of Alpine Divide, we assume that 305 m (1000 ft) of Triassic Chinle Group and

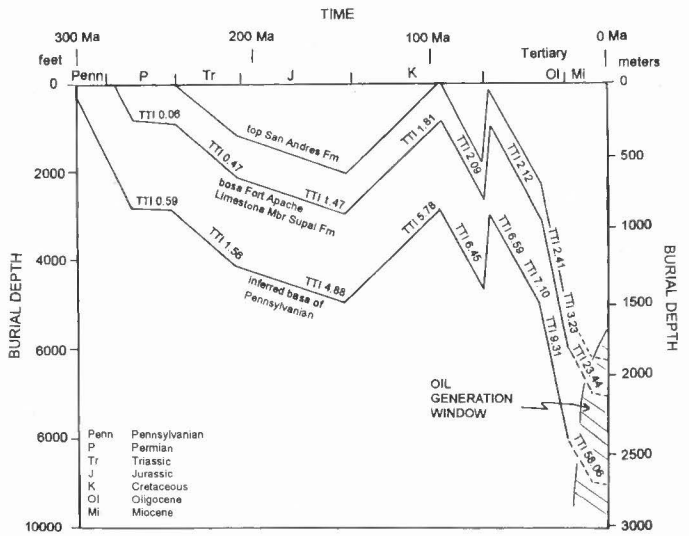

FIGURE 2.54. Lopatin maturation model for a hypothetical late-Tertiary graben with pre-Miocene Alpine Divide subsurface geology. Time-temperature index, heat flow, thermal conductivity, and surface temperature assumptions as in Fig 2.53.

305 m (1000 ft) of Jurassic sediments were deposited over the area. Uplift and erosion associated with the sub-Late Cretaceous unconformity stripped these rocks from the section along with more than two thirds of an estimated 91 m (300 ft) thickness of Permian San Andres Formation (Witcher, et al., this volume). Most of the inferred 610 m (2000 ft) thickness of Cretaceous rocks were stripped beneath a Laramide unconformity. Also, 610 m (2000 ft) of pre-Fort Apache Limestone Member of the Supai Formation rocks were included to investigate possible maturation indices in Pennsylvanian rocks, if present in the subsurface below the total depth of the Alpine 1/Divide corehole at 1373 m (4505 ft).

In Model 1, rapid burial occurred from the beginning of the Eocene until the end of the Oligocene, followed by uplift and erosion (Witcher, et al., this volume) (Fig. 2.53). Waples (1980) presented evidence that the onset of oil generation begins at a TTI of 15. Base of the Fort Apache Limestone Member of the Supai Formation reached a TTI value of 6. If the model thicknesses for the Triassic, Jurassic and Cretaceous rocks are doubled, the Fort Apache Limestone TTI remains below the TTI 15 oil-generation threshold at TTI 9.7. Model 1 temperature at the base of the Fort Apache is 74.2° C, compared to the measured temperature of 77.2° C in the Alpine 1/Federal. If a thick Pennsylvanian section is present, Model 1 predicts a TTI of 21, indicating potential for oil generation beginning after 15 to 10 Ma. No oil generation is predicted for the cored section in the Alpine 1/Federal. Oil shows in the corehole are either related to intrusive heating or represent migrated oil.

Model 2 is the same as Model 1 until the end of the Oligocene. Instead of uplift and erosion, the entire Eocene to Oligocene sequence is preserved and buried under an additional 305 m (1000 ft) of Miocene clastic sediments (Fig. 2.54). In Model 2, the TTI for the base of the Fort Apache Limestone Member is within the oil-generation window at 23.4. Potentially more significant, the Pennsylvanian TTI is 58. Waples' (1980) research indicates that peak oil generation occurs at a TTI of 75. If a heat flow of 70 mW/m^2 is used for the post-Oligocene instead of the 90 mW/m^2 value for Alpine Divide, the Fort Apache Limestone TTI is 19 and the Pennsylvanian TTI is 28. Permian and Pennsylvanian source rocks enter the oil-generation window after 15 to 10 Ma.

Three different basaltic intrusions are present in the Supai Formation (Witcher et al., this volume). Two intrusive bodies are near 30.5 m (100 ft) thickness. The third intrusion thickness is unknown. Each intrusion is assumed to have cooled to roughly ambient temperature before the next intrusion. A conductive model is used to investigate the potential role in oil generation by the basaltic intrusions (Carslaw and Jaeger, 1962, p. 58-62; Lachenbruch, 1976, p. 775, fig. 7b). A sill, 30.5 m (100 ft) thick, of semi-infinite lateral extent is instantaneously intruded with a top at 1298 m (4260 ft) depth. The sill is allowed to cool conductively with a constant pre-intrusive land surface temperature. Thermal diffusivities of the intrusion and the country rock are assumed to be the same. This assumption is adequate for a good approximation (Jaeger, 1968, p. 505). In order to account for latent heat of fusion, an additional 300°C is added to the initial intrusive temperature of 1200°C (Jaeger, 1964, 1968). No magma convection is allowed in the model. The model is not suitable for intrusions that represent conduits for volcanism on the surface. A no-flow assumption after the initial magma intrusion is reasonable because chilled margins are observed in the core. Magma convection or flow would tend to melt country rock (and chilled margins) and result in more intense thermal disturbance of the country rock (Huppert and Sparks, 1989).

The thermal histories of several sites, ranging from 15 to 213 m (50 to 700 ft), over the top of the cooling sill are modeled (Fig. 2.55). Around 30,000 yrs after the intrusion event, the country rock cools to within 10°C of pre-intrusion ambient temperature. Application of the Lopatin maturation model indicates oil-generation potential during the first 100 years in a rock volume, extending upward between 0 and 30.5 m (0 and 100 ft) above the sill. An initial country rock temperature of 70°C was added to the anomalous intrusive temperature profile in order to estimate maturation indices. If hydrothermal convection in the country rock above the sill occurred, cooling times would be faster and temperatures would be lower, possibly eliminating oil generation. A 30.5 m (100 ft) thick model for a vertical dike at 1298 m (4260 ft) would give temperatures similiar to the sill in locations situated perpendicular to the dike (parallel to land surface). However, a concordant sill has potential to mature a much greater volume of source rock compared to a cross-cutting dike.

The Lopatin oil maturation models are first-order approximations. Hunt and Hennet (1992) showed that kerogen type has a strong influence on maturation rates. For instance, high-sulfur kerogens have faster kinetics, resulting from the lower activation energies of carbon-sulfur bonds. Geochemical analysis of kerogen types in the Paleozoic source rocks will allow a more rigorous Arrhenius-equation approach to determine petroleum maturation indices. Hydrothermal convection can enhance petroleum genesis. At high temperatures (>100°C), hydrocarbons become exponentially more soluble in water, which allows rapid transport away from destructive thermal processes near intrusions (Simoneit, 1983). Also, Barker (1989) showed that Arrhenius reaction rates for hydrothermal systems and in zones along intrusive contacts are much faster than burial generation rates modeled by the Lopatin approach.

Preliminary thermal maturation models indicate the best potential for petroleum genesis is in Pennsylvanian and Permian rocks, which may be preserved in the deeper pre-mid-Tertiary basins and in the late Tertiary grabens along the Colorado Plateau (Mogollon slope) and the Transition zone (Datil-Mogollon section) of the Basin and Range Province. The models indicate that Permian and Cretaceous source rocks outside deeper basins and grabens probably have not entered the oil-generation window. Limited-volume maturation zones may include eruptive centers for late Tertiary basaltic volcanism. Conduits (volcanic

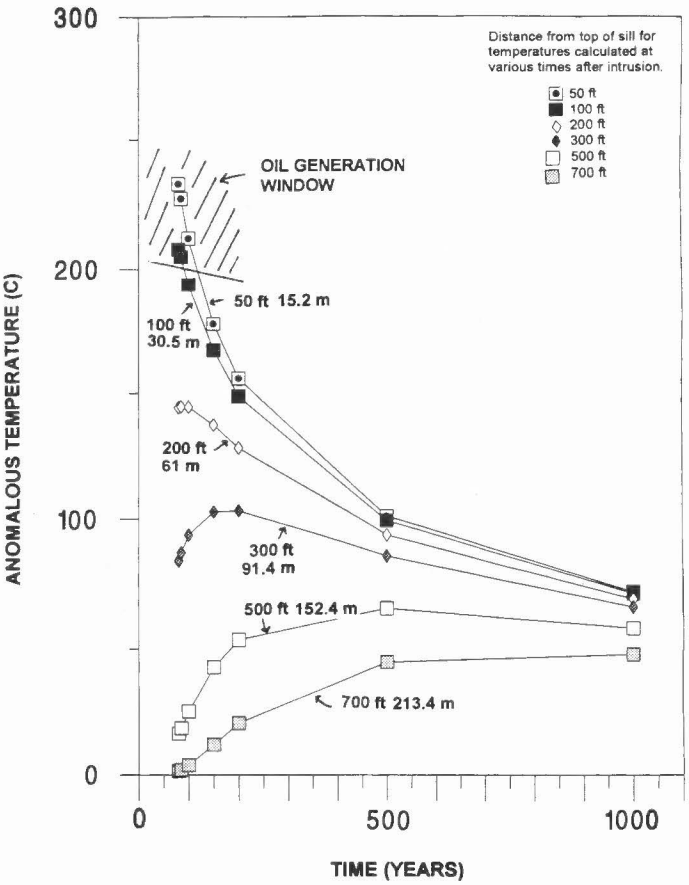

FIGURE 2.55. Temperature versus time cooling model for a sill, 30.5 m (100 ft) thick. Curves show time-temperature relations at varying distances from sill. Intrusion temperature is 1500°C (1200°C plus 300°C to correct for latent heat released during magma crystallization). Thermal diffusivity is 0.0001 m^2/sec. Model based upon Carslaw and Yeager (1959, p. 58-62) and Lachenbruch et al. (1976, p. 775, fig. 7b).

vents) for magma flow could give rise to sustained thermal disturbance for maturation of Paleozoic source rocks and possibly local hydrothermal oil generation. Preliminary analysis indicates that the oil shows in the Alpine 1/Federal borehole are probably the result of very local maturation due to basaltic intrusions. Even though piezometric levels in the corehole appear to decrease with depth, upward migration of oil from depth is not ruled out. In any case, oil generation in the region began after 15 to 10 Ma.

GEOTHERMAL POTENTIAL OF THE ALPINE DIVIDE AREA

James C. Witcher[1], Chandler A. Swanberg[2] and W. Richard Hahman[3]

[1]New Mexico State University, Southwest Technology Development Institute, Las Cruces, NM, 88003; [2]Consultant, 5478, E. Cholla St., Scottsdale, AZ 85254; [3]Consultant, 780 Suzanne Ave., Las Cruces, NM 88005

Geothermal energy as hydrothermal resources or naturally occurring hot water and steam currently provides commercially competitive electrical power and direct heat for space heating, greenhouses, industrial processing, aquaculture, food processing and many other uses that require low-grade heat. Excluding the use of heat pumps, direct-use geothermal heating in the United States at 1026 sites accounted for 18,270 trillion Btu/yr with an installed capacity of 5862 million Btu per hr (MMBTU) in 1988 from mostly low-to-intermediate temperature (<150°C) hydrothermal resources (Lienau, 1988). The installed capacity of geothermal electrical power generation in the United States was 2770 MWe in 1989 from mostly high-temperature (>150°C) hydrothermal resources (Rannels and McLarty, 1990).

However, the largest potentially accessible terrestrial energy resource is hot dry rock (HDR) geothermal. The higher grade (basement gradients > 45°C/km) HDR resource base in the United States is estimated at 650,000 Quads or the oil equivalent of about 11,000 Prudhoe Bays (118 trillion barrels of oil) (Tester et al., 1989). Hot dry rock (HDR) geothermal energy is a method of extracting natural heat from "dry" impermeable rock (conductive thermal regime). As originally conceived by scientists and engineers at Los Alamos National Laboratory, heat is extracted from relatively impermeable rock by artificially fracturing a hot volume of rock and introducing water into the man-made fracture system with an injection well. A second well produces the heated water from the fracture reservoir for use at the surface. The HDR concept and a degree of technical feasibility has been demonstrated at Fenton Hill, New Mexico. On the other hand, commercial feasibility has not been demonstrated for the general use of HDR.

Electrical power production and direct-use applications are possible end uses of HDR. Considering fossil fuel costs, a site with near-term HDR potential requires an area with currently high electrical or utility fuel costs. Because drilling costs increase non-linearly with depth, high temperatures at relatively shallow depth are required for economic energy extraction.

A temperature versus depth plot for the Alpine 1/Federal borehole shows that temperature gradients decrease with depth (Fig. 2.56). Increasing rock thermal conductivity accounts for the lower temperature gradients. Clay-rich sediments in the upper portion of the hole have relatively low thermal conductivity (<2.0 W/mK). Quartzose sandstones and carbonate rocks in the lower portion of the hole have high thermal conductivity (>2.0 W/mK). A preliminary heat flow of 90 mW/m^2 is reported for the hole (J. H. Sass, personal commun., 1994). Thermal conductivity constraints indicate that a gradient of over 35°C/km probably cannot occur in Precambrian basement. For instance, granitic rocks typically have a thermal conductivity ranging from 2.6 to 3.6 W/mK (Roy et al., 1981, p. 454, fig. 12-47).

Tester and Herzog (1990) defined three grades of HDR resources for the purpose of investigating feasibility. A high-grade resource has a gradient above 80°C/km; a mid-grade resource has a gradient of 50°C/km; and a low-grade resource has a gradient of 30°C/km. Within this framework, the Alpine area falls into the low-grade category.

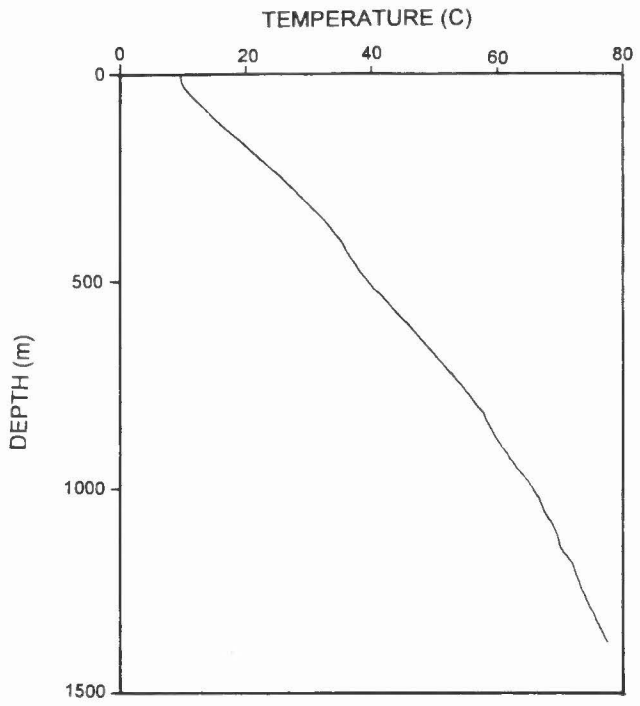

FIGURE 2.56. Temperature versus depth for the Alpine 1/Federal corehole at Alpine Divide.

Tester and Herzog (1990) modeled the cost of electricity with current technology on a per-KWe installed basis. With a 40°C/km gradient, costs for electricity are 12 to 18 cents per kilowatt-hour. These costs are unlikely to be economic for the foreseeable future in eastern Arizona.

Tester and Herzog (1990) also modeled the costs for direct-use HDR, based upon a heat supply of one million Btu per hour (MMBTU). Costs for direct use are a little more attractive. The key parameters involved with direct-use HDR in the Alpine area are heating loads and natural gas availibility. Climate in the area requires space heating for much of the year so that potentially large heating loads may exist. Inexpensive natural gas is not available. Direct-use space heating, using the 40°C/km gradient model of Tester and Herzog (1990) indicates a $4 to $7 per MMBTU cost. This cost may be marginally economic for very large space-heating requirements. However, with natural gas costs in the $3 to $5 MMBTU range ($5 to $7 MMBTU with boiler inefficiencies), it is unlikely that commercial enterprises would relocate for industrial process heat or space heat.

The best potential HDR geothermal application is a district heating system for Alpine. Costs per MMBTU for HDR will be higher than model costs because additional costs would be incurred for distribution lines. Loss of circulation during coring of the Permian San Andres, Glorieta and Supai formations indicates potential for production of 70°C water (conventional geothermal) from depths between 915 and 1220 m (3000 and 4000 ft), if these units are present beneath Alpine (Witcher et al., this volume). However, the costs to drill, complete and test a large diameter production well to 1220 m (4000 ft) could approach a million dollars. Additional capital costs would be incurred for distribution lines and possibly an injection well. A study of heating loads and engineering feasibility is required to assess the direct-use economics at Alpine. However, for HDR and conventional geothermal to compete with current propane use in Alpine, the system would probably have to operate as a utility and have initial capital costs subsidized.

129.4 Roadcuts in Spears Group next 2.0 mi. Sandstones and debris-flow deposits resemble Pueblo Creek Formation above andesite of Dry Leggett Canyon in Bull Basin quadrangle (Ratté, 1989), and likely are correlative of same. **2.2**

131.6 Road to Big Lake on right. Continue straight on US-666. **0.5**

132.1 Valley and lake on right is in headwater drainage of San Francisco River (Fig. 2.57). **0.2**

132.3 Spears Group on left. **1.0**

133.3 Junction with road to Luna, New Mexico (US-180) in Alpine, Arizona.

End second-day road log.

FIGURE 2.57. View south of town of Alpine, Arizona and headwater drainage of San Francisco River.

Morning fog rolls over the central Sawtooth Mountains, view to north from US-60. Black and white print by De Mar Co. Photographics from color slide © Kelly D. Gatlin, La Luz Photography.